

Bayesian causal inference in probit graphical models

Federico Castelletti & Guido Consonni *

Abstract

We consider a binary response which is potentially affected by a set of continuous variables. Of special interest is the causal effect on the response due to an intervention on a specific variable. The latter can be meaningfully determined on the basis of observational data through suitable assumptions on the data generating mechanism. In particular we assume that the joint distribution obeys the conditional independencies (Markov properties) inherent in a Directed Acyclic Graph (DAG), and the DAG is given a causal interpretation through the notion of interventional distribution. We propose a DAG-probit model where the response is generated by discretization through a random threshold of a continuous latent variable and the latter, jointly with the remaining continuous variables, has a distribution belonging to a zero-mean Gaussian model whose covariance matrix is constrained to satisfy the Markov properties of the DAG. Our model leads to a natural definition of causal effect conditionally on a given DAG. Since the DAG which generates the observations is unknown, we present an efficient MCMC algorithm whose target is the posterior distribution on the space of DAGs, the Cholesky parameters of the concentration matrix, and the threshold linking the response to the latent. Our end result is a Bayesian Model Averaging estimate of the causal effect which incorporates parameter, as well as model, uncertainty. The methodology is assessed using simulation experiments and applied to a gene expression data set originating from breast cancer stem cells.

1 Introduction

We consider a system of random quantities, which includes a binary response as well as a collection of continuous variables, and address the problem of determining the causal effect on the response due to an intervention on a given variable. A causal question involves the data generating mechanism after an intervention is applied to the system, and must be carefully distinguished from traditional conditioning of probability theory (Pearl, 2009, Section 2.4). The gold standard for addressing causal questions is represented by randomized controlled experiments; the latter however are not always available because they may be unethical, infeasible,

*Department of Statistical Sciences, Università Cattolica del Sacro Cuore, Milan, federico.castelletti@unicatt.it, guido.consonni@unicatt.it

time consuming or expensive (Maathuis & Nandy, 2016). By contrast, *observational* data, that is observations produced without exogenous perturbations of the system, are widely available and often plentiful. The challenge is then to infer causal effects based on observational data alone. To achieve this goal, it is crucial to set up a suitable conceptual framework which is able to address causal questions; in particular the notion of *joint distribution* for a collection of random variables can only address concepts linked to association, so much so that, by converse, “a causal concept is any relationship that cannot be defined from the distribution alone” (Pearl, 2009, Section 2).

A very useful framework to bridge the gap between the observational and the experimental domains is represented by the Directed Acyclic Graph (DAG), or its allied concept of Structural Equation Model (SEM); see Pearl (1995) and Pearl (2000). DAGs have been extensively used to construct statistical models embodying conditional independence relations (Lauritzen, 1996). Applications are numerous especially in genomics; see for instance Friedman (2004) and Friedman & Koller (2003). With observational data, conditional independence relations will drive inference on DAG and parameter space. On the other hand, the additional syntax and semantics of *causal* DAGs (Pearl, 2000) will be instrumental to define the notion of causal effect.

As in standard probit regression (Albert & Chib, 1993), we assume that the observable binary response is the result of a discretization of a continuous *latent* variable. Next, for a given DAG, we model all continuous random variables, along with the latent, as a multivariate Gaussian family satisfying the corresponding Markov property. We call the resulting setup a *DAG-probit* model, and provide a definition of causal effect on the response which is predicated on a given DAG through the notion of *interventional* distribution (Pearl, 2000). However the structure of the DAG is usually unknown, and this must be taken into account because different DAGs will typically induce distinct causal effects; see the review paper Maathuis & Nandy (2016) and Castelletti & Consonni (2020a) for a Bayesian approach.

In this work we extend the notion of interventional distribution and causal effect (Pearl, 2000; Maathuis et al., 2009) to DAG-probit models. Specifically, we propose a Bayesian method which jointly performs DAG-model determination as well as inference of causal effects in the presence of a binary response. From a computational viewpoint we introduce an MCMC scheme to sample from the joint posterior of models (DAGs) and model-dependent parameters (causal effects) which we implement through an efficient PAS algorithm (Godsill, 2012). The rest of the paper is organized as follows. In Section 2 we review DAG-Gaussian models and define the DAG-probit model. In Section 3 we present the structure of the interventional distribution in its general form, then specialize it to the Gaussian case, and finally extend the definition of causal effect to DAG-probit models. Section 4 presents our Bayesian methodology with particular emphasis on priors for model parameters. An MCMC algorithm for posterior inference on models, parameters and hence causal effects is presented in Section 5. We evaluate the proposed

methodology through simulation studies in Section 6, and then apply it to a data set on gene expression measurements derived from breast cancer stem cells (Section 7). Finally a few points for discussion are presented in Section 8. Some theoretical results as well as additional simulation outputs are reported in the Supplementary material (Castelletti & Consonni, 2020b).

2 Model formulation

In this section we first provide some background material on Gaussian DAG-models with special emphasis on their parameterization (Section 2.1). Next we present our DAG-probit model (Section 2.2). Both sections deal with the likelihood, while choices of prior distributions are discussed in Section 4.

2.1 Gaussian DAG-models

Let $\mathcal{D} = (V, E)$ be a DAG, where $V = \{1, \dots, q\}$ is a set of vertices (or nodes) and $E \subseteq V \times V$ a set of edges whose elements are $(u, v) \equiv u \rightarrow v$, such that if $(u, v) \in E$ then $(v, u) \notin E$. In addition, \mathcal{D} contains no cycles, that is paths of the form $u_0 \rightarrow u_1 \rightarrow \dots \rightarrow u_k$ where $u_0 \equiv u_k$. For a given node v , if $u \rightarrow v \in E$ we say that u is a *parent* of v (conversely v is a *child* of u). The parent set of v in \mathcal{D} is denoted by $\text{pa}(v)$, the set of children by $\text{ch}(v)$. Moreover, we denote by $\text{fa}(v) = v \cup \text{pa}(v)$ the *family* of v in \mathcal{D} . For further theory and notation on DAGs we refer to Lauritzen (1996).

We consider a collection of random variables (X_1, \dots, X_q) and assume that their joint probability density function $f(\mathbf{x})$ is Markov w.r.t. \mathcal{D} , so that it admits the following factorization

$$f(x_1, \dots, x_q) = \prod_{j=1}^q f(x_j | \mathbf{x}_{\text{pa}(j)}). \quad (1)$$

In this section, as well as in Section 3, we reason *conditionally* on a given DAG \mathcal{D} without an explicit conditioning in the notation we use. In Section 4 we will instead deal with model (DAG) uncertainty and will reinstate \mathcal{D} in our notation.

If the joint distribution is Gaussian with mean equal to zero, we write

$$X_1, \dots, X_q | \mathbf{\Omega} \sim \mathcal{N}_q(\mathbf{0}, \mathbf{\Omega}^{-1}), \mathbf{\Omega} \in \mathcal{P}_{\mathcal{D}} \quad (2)$$

where $\mathbf{\Omega} = \mathbf{\Sigma}^{-1}$ is the precision matrix, and $\mathcal{P}_{\mathcal{D}}$ is the space of symmetric positive definite (s.p.d.) precision matrices Markov w.r.t. \mathcal{D} . For a Gaussian DAG-model factorization (1) becomes

$$f(x_1, \dots, x_q | \mathbf{\Omega}) = \prod_{j=1}^q d\mathcal{N}(x_j | \mu_j(\mathbf{x}_{\text{pa}(j)}), \sigma_j^2), \quad (3)$$

where $d\mathcal{N}(\cdot | \mu, \sigma^2)$ denotes the normal density having mean μ and variance σ^2 . The assumption of normality guarantees that the model is *faithful* to the DAG, that is all and only those conditional independencies embodied in the joint distribution can be read-off from the graph using the Markov property; see also [Spirites et al. \(2000\)](#).

Without loss of generality, we assume a *parent ordering* of the nodes which numerically labels the variables so that $i > j$ whenever j is a child of i . A parent ordering always exists, although it is not unique in general. We also remark that a parent ordering is specific to any given DAG under consideration and may change if alternative DAGs are entertained. Importantly, it only represents a convenient device to specify a prior on the parameter space; see Section 4 where we also show that the choice of the parent ordering does not affect the prior assigned to model parameters.

Moreover, we declare node 1, which cannot have children, to be the (latent) outcome variable. Equation (3) can be also written as a *structural equation model*

$$\mathbf{L}^\top (X_1, \dots, X_q)^\top = \boldsymbol{\varepsilon}, \quad (4)$$

where because of the assumed parent ordering \mathbf{L} is a (q, q) *lower-triangular* matrix of coefficients, $\mathbf{L} = \{\mathbf{L}_{ij}, i \geq j\}$, such that $\mathbf{L}_{ij} \neq 0$ if and only if $i \rightarrow j$ and $\mathbf{L}_{ii} = 1$. Moreover, $\boldsymbol{\varepsilon}$ is a $(q, 1)$ vector of error terms, $\boldsymbol{\varepsilon} \sim \mathcal{N}_q(\mathbf{0}, \mathbf{D})$, where $\mathbf{D} = \text{diag}(\boldsymbol{\sigma}^2)$ and $\boldsymbol{\sigma}^2$ is the $(q, 1)$ vector of *conditional* variances whose j -th element is $\sigma_j^2 = \text{Var}(X_j | \mathbf{x}_{\text{pa}(j)}, \boldsymbol{\Omega})$. From (4) it follows that

$$\boldsymbol{\Omega} = \mathbf{L} \mathbf{D}^{-1} \mathbf{L}^\top. \quad (5)$$

We refer to Equation (5) as the *modified Cholesky decomposition* of $\boldsymbol{\Omega}$. Let now $\prec j \succ = \text{pa}(j)$ and $\prec j] = \text{pa}(j) \times j$. Representation (5) induces a re-parametrization of $\boldsymbol{\Omega}$ in terms of the Cholesky parameters $\{(\sigma_j^2, \mathbf{L}_{\prec j]}), j = 1, \dots, q\}$, where

$$\mathbf{L}_{\prec j]} = -\boldsymbol{\Sigma}_{\prec j \succ} \boldsymbol{\Sigma}_{\prec j]}^{-1}, \quad \sigma_j^2 = \boldsymbol{\Sigma}_{jj | \text{pa}(j)};$$

see also [Cao et al. \(2019\)](#). Accordingly, Equation (3) can be written as

$$f(x_1, \dots, x_q | \mathbf{D}, \mathbf{L}) = \prod_{j=1}^q d\mathcal{N}(x_j | -\mathbf{L}_{\prec j]}^\top \mathbf{x}_{\text{pa}(j)}, \sigma_j^2), \quad (6)$$

with the understanding that the conditional expectation of X_j in (6) is zero whenever $\text{pa}(j)$ is the empty set.

2.2 DAG-probit models

We introduce in this section the general form of a *DAG-probit model*. We assume that the joint distribution of (X_1, X_2, \dots, X_q) is Gaussian and Markov w.r.t. \mathcal{D} so that its density is as in

(6). Recall that X_1 is latent and we are only allowed to observe the binary variable $Y \in \{0, 1\}$. Specifically, for a given threshold $\theta_0 \in (-\infty, +\infty)$, we assume that

$$Y = \begin{cases} 1 & \text{if } X_1 \in [\theta_0, +\infty), \\ 0 & \text{if } X_1 \in (-\infty, \theta_0). \end{cases} \quad (7)$$

Combining (6) with (7), the joint density of (Y, X_1, \dots, X_q) becomes

$$\begin{aligned} f(y, x_1, \dots, x_q \mid \mathbf{D}, \mathbf{L}, \theta_0) &= f(x_1, \dots, x_q \mid \mathbf{D}, \mathbf{L}) \cdot \mathbb{1}(\theta_{y-1} < x_1 \leq \theta_y) \\ &= \left\{ \prod_{j=1}^q d\mathcal{N}(x_j \mid -\mathbf{L}_{\prec j}^\top \mathbf{x}_{\text{pa}(j)}, \sigma_j^2) \right\} \cdot \mathbb{1}(\theta_{y-1} < x_1 \leq \theta_y), \end{aligned} \quad (8)$$

where $\theta_{-1} = -\infty, \theta_1 = +\infty$. Equation (8) defines a (Gaussian) *DAG-probit model*. A related expression appears in Guo et al. (2015) who model a multivariate distribution of ordered categorical variables through a collection of Gaussian random variables Markov with respect to an undirected graphical model. Now recall from (6) that the conditional distribution of the latent variable X_1 is $\mathcal{N}(-\mathbf{L}_{\prec 1}^\top \mathbf{x}_{\text{pa}(1)}, \sigma_1^2)$ and, as in standard probit regression, we set $\sigma_1^2 = 1$ for identifiability reasons.

Finally, by considering n independent samples $(y_i, x_{i,2}, \dots, x_{i,q})$, $i = 1, \dots, n$, from (8), the *augmented* likelihood can be written as

$$\begin{aligned} f(\mathbf{y}, \mathbf{X} \mid \mathbf{D}, \mathbf{L}, \theta_0) &= \prod_{i=1}^n f(x_{i,1}, \dots, x_{i,q} \mid \mathbf{D}, \mathbf{L}) \cdot \mathbb{1}(\theta_{y_i-1} < x_{i,1} \leq \theta_{y_i}) \\ &= \prod_{j=1}^q d\mathcal{N}_n(\mathbf{X}_j \mid -\mathbf{X}_{\text{pa}(j)} \mathbf{L}_{\prec j}, \sigma_j^2 \mathbf{I}_n) \cdot \left\{ \prod_{i=1}^n \mathbb{1}(\theta_{y_i-1} < x_{i,1} \leq \theta_{y_i}) \right\}, \end{aligned} \quad (9)$$

where $\mathbf{y} = (y_1, \dots, y_n)^\top$, \mathbf{X} is the (n, q) augmented data matrix, and \mathbf{X}_A is the submatrix of \mathbf{X} corresponding to the set A of columns of \mathbf{X} .

3 Causal effects

Consider the joint density of the random vector (X_1, \dots, X_q) Markov w.r.t. a DAG which factorizes as in (1); the latter is referred to as the *observational* (or *pre-intervention*) distribution.

We now introduce the notion of *intervention*. A deterministic intervention on variable X_s , $s \in \{2, \dots, q\}$ is denoted by $\text{do}(X_s = \tilde{x})$ and consists in setting X_s to the value \tilde{x} . The *post-intervention* density of (X_1, \dots, X_q) is then obtained using the truncated factorization

$$f(x_1, \dots, x_q \mid \text{do}(X_s = \tilde{x})) = \begin{cases} \prod_{j=1, j \neq s}^q f(x_j \mid \mathbf{x}_{\text{pa}(j)})|_{x_s=\tilde{x}} & \text{if } x_s = \tilde{x}, \\ 0 & \text{otherwise,} \end{cases} \quad (10)$$

where, importantly, each term $f(x_j | \cdot)$ in (10) is the corresponding (pre-intervention) conditional distribution of Equation (1); see Pearl (2000). We emphasize that the post-intervention density $f(x_1, \dots, x_q | \text{do}(X_s = \tilde{x}))$ is conceptually distinct from the usual *conditional* density $f(x_1, \dots, x_q | X_s = \tilde{x})$, which arises out of passive observation of $X_s = \tilde{x}$. An important feature of Equation (10) is that the data generating system is “stable” under exogenous interventions, in the sense that only the local component distribution $f(x_s | \mathbf{x}_{\text{pa}(s)})$ is affected by the intervention and effectively reduces to a point mass on \tilde{x} . All the remaining terms are immune to the intervention and thus remain the same. The post-intervention distribution of the (latent) response X_1 is then obtained by integrating (10) w.r.t. x_2, \dots, x_q which simplifies to

$$f(x_1 | \text{do}(X_s = \tilde{x})) = \int f(x_1 | \tilde{x}, \mathbf{x}_{\text{pa}(s)}) f(\mathbf{x}_{\text{pa}(s)}) d\mathbf{x}_{\text{pa}(s)}; \quad (11)$$

see also Pearl (2000, Theorem 3.2.2).

We now move back to the Gaussian setting of Section 2.1, and assume that $(X_1, X_2, \dots, X_q) | \Sigma \sim \mathcal{N}_q(\mathbf{0}, \Sigma)$, where the covariance matrix Σ is Markov w.r.t. to the underlying DAG. The post-intervention distribution of X_1 can thus be written as

$$\begin{aligned} f(x_1 | \text{do}(X_s = \tilde{x}), \Sigma) &= \int f(x_1 | \tilde{x}, \mathbf{x}_{\text{pa}(s)}, \Sigma) \cdot f(\mathbf{x}_{\text{pa}(s)} | \Sigma) d\mathbf{x}_{\text{pa}(s)} \\ &= \int d\mathcal{N}(x_1 | \gamma_s \tilde{x} + \boldsymbol{\gamma}^\top \mathbf{x}_{\text{pa}(s)}, \delta_1^2) \cdot d\mathcal{N}(\mathbf{x}_{\text{pa}(s)} | \mathbf{0}, \Sigma_{\text{pa}(s), \text{pa}(s)}) d\mathbf{x}_{\text{pa}(s)}, \end{aligned} \quad (12)$$

where $\delta_1^2 = \text{Var}(X_1 | X_s = \tilde{x}, \mathbf{x}_{\text{pa}(s)}, \Sigma)$. The following Proposition gives the analytic form of the post-intervention distribution of X_1 .

Proposition 3.1. *Let $(X_1, X_2, \dots, X_q) | \Sigma \sim \mathcal{N}_q(\mathbf{0}, \Sigma)$ and consider the do operator $\text{do}(X_s = \tilde{x})$, $s \in \{2, \dots, q\}$. Then the post-intervention distribution of X_1 is*

$$f(x_1 | \text{do}(X_s = \tilde{x}), \Sigma) = d\mathcal{N}\left(x_1 | \gamma_s \tilde{x}, \frac{\delta_1^2}{1 - (\boldsymbol{\gamma}^\top \mathbf{T}^{-1} \boldsymbol{\gamma}) / \delta_1^2}\right),$$

where

$$\begin{aligned} \delta_1^2 &= \Sigma_{1 | \text{fa}(s)}, \\ (\gamma_s, \boldsymbol{\gamma}^\top)^\top &= \Sigma_{1, \text{fa}(s)} (\Sigma_{\text{fa}(s), \text{fa}(s)})^{-1}, \\ \mathbf{T} &= (\Sigma_{\text{pa}(s), \text{pa}(s)})^{-1} + \frac{1}{\delta_1^2} \boldsymbol{\gamma} \boldsymbol{\gamma}^\top, \end{aligned}$$

with the understanding that node s occupies the first position in the set $\text{fa}(s)$.

Proof. See Supplementary material (Castelletti & Consonni, 2020b). □

The previous reasoning considered the intervention distribution of the latent response variable X_1 following $\text{do}(X_s = \tilde{x})$. Typically distribution (11) is summarized by its expected value $\mathbb{E}(X_1 | \text{do}(X_s = \tilde{x}))$. When X_s is continuous, one can define the (total) causal effect as the

derivative of $\mathbb{E}(X_1 | \text{do}(X_s = x))$ w.r.t. x evaluated at \tilde{x} : this is especially convenient when the expectation is linear, as in the Gaussian case (12), because the causal effect admits a simple interpretation: it corresponds to the “regression parameter” γ_s associated to variable X_s (Maathuis et al., 2009). Our interest however lies in the observable response variable Y , and therefore we aim to evaluate $\mathbb{E}(Y | \text{do}(X_s = \tilde{x}), \mathbf{\Sigma}, \theta_0)$. We thus obtain

$$\begin{aligned} \mathbb{E}(Y | \text{do}(X_s = \tilde{x}), \mathbf{\Sigma}, \theta_0) &= \Pr(Y = 1 | \text{do}(X_s = \tilde{x}), \mathbf{\Sigma}, \theta_0) \\ &= \Pr(X_1 \geq \theta_0 | \text{do}(X_s = \tilde{x}), \mathbf{\Sigma}) \\ &= 1 - \Phi\left(\frac{\theta_0 - \gamma_s \tilde{x}}{\tau_1}\right) \equiv \beta_s(\tilde{x}, \mathbf{\Sigma}, \theta_0), \end{aligned} \quad (13)$$

where $\Phi(\cdot)$ denotes the c.d.f. of a standard normal and $\tau_1^2 = \delta_1^2 / (1 - (\boldsymbol{\gamma}^\top \mathbf{T}^{-1} \boldsymbol{\gamma}) / \delta_1^2)$. One could then compute the partial derivative of $\mathbb{E}(Y | \text{do}(X_s = \tilde{x}), \mathbf{\Sigma}, \theta_0)$ w.r.t x evaluated at \tilde{x} , and obtain $\phi(\theta_0 - \gamma_s \tilde{x} / \tau_1) \gamma_s / \tau_1$, where $\phi(\cdot)$ is the density function of a standard normal. This however would still depend on \tilde{x} . For this reason, and because (13) enjoys an intuitive interpretation being a probability, we will simply denote $\Pr(Y = 1 | \text{do}(X_s = \tilde{x}), \mathbf{\Sigma}, \theta_0)$ at the causal effect on Y due to an intervention $\text{do}(X_s = \tilde{x})$. Finally, we remark that the causal effect of $\text{do}(X_s = \tilde{x})$ on Y , besides being a function of the value \tilde{x} , depends on θ_0 as well as on the covariance matrix $\mathbf{\Sigma}$, where the latter is constrained to be Markov w.r.t. the underlying DAG.

4 Bayesian inference

In this section we introduce priors for $(\boldsymbol{\Omega}, \theta_0, \mathcal{D})$, which we structure as $p(\boldsymbol{\Omega}, \theta_0, \mathcal{D}) = p(\boldsymbol{\Omega} | \mathcal{D})p(\mathcal{D})p(\theta_0)$. Further distributional results useful for our MCMC scheme of Section 5 are also presented. We briefly preview here the essential features.

To start with, consider $p(\boldsymbol{\Omega} | \mathcal{D})$, $\boldsymbol{\Omega} \in \mathcal{P}_{\mathcal{D}}$. We first proceed to the re-parameterization $\boldsymbol{\Omega} \mapsto (\mathbf{D}, \mathbf{L})$ presented in Subsection 2.1, and specify a DAG-Wishart prior (Cao et al., 2019) on the Cholesky parameters (\mathbf{D}, \mathbf{L}) . We achieve this goal using a highly parsimonious elicitation procedure, which we detail in Section 4.1. For the unknown threshold $\theta_0 \in (-\infty, +\infty)$, we assume a uniform prior, so that $p(\theta_0) \propto 1$ (Section 4.3). Finally, a prior on DAG \mathcal{D} is assigned through independent Bernoulli distributions on the elements of the skeleton of \mathcal{D} (Section 4.2).

4.1 Prior on the Cholesky parameters

Consider first a DAG $\mathcal{D} = (V, E)$ which is *complete*, so that the precision matrix $\boldsymbol{\Omega}$ is unconstrained. A standard conjugate prior is the Wishart distribution, $\boldsymbol{\Omega} \sim \mathcal{W}_q(a, \mathbf{U})$ having expectation $a\mathbf{U}^{-1}$, where $a > q - 1$ and \mathbf{U} is a s.p.d. matrix. The induced prior on the Cholesky parameters consistent with the DAG parent ordering is such that the node parameters

$(\sigma_j^2, \mathbf{L}_{\prec j}]$, $j = 1, \dots, q$, are independent with distribution

$$\begin{aligned}\sigma_j^2 &\sim \text{I-Ga}\left(\frac{a_j}{2} - \frac{|\text{pa}(j)|}{2} - 1, \frac{1}{2}\mathbf{U}_{jj|\prec j}\right), \\ \mathbf{L}_{\prec j} | \sigma_j^2 &\sim \mathcal{N}_{|\text{pa}(j)|}\left(-\mathbf{U}_{\prec j}^{-1}\mathbf{U}_{\prec j}, \sigma_j^2\mathbf{U}_{\prec j}^{-1}\right),\end{aligned}\quad (14)$$

where $|A|$ is the number of elements in the set A , $a_j = a + q - 2j + 3$; see [Ben-David et al. \(2015, Supplemental B\)](#). The symbol $\text{I-Ga}(a, b)$ stands for an Inverse-Gamma distribution with shape $a > 0$ and rate $b > 0$ having expectation $b/(a - 1)$ ($a > 1$). In absence of substantive prior information, a standard choice for the hyperparameter \mathbf{U} , hereinafter adopted, is $\mathbf{U} = g\mathbf{I}_q$, where $g > 0$ and \mathbf{I}_q is the (q, q) identity matrix. It is straightforward to show that (14) reduces to

$$\begin{aligned}\sigma_j^2 &\sim \text{I-Ga}\left(\frac{a_j}{2} - \frac{|\text{pa}(j)|}{2} - 1, \frac{1}{2}g\right), \\ \mathbf{L}_{\prec j} | \sigma_j^2 &\sim \mathcal{N}_{|\text{pa}(j)|}\left(\mathbf{0}, \frac{1}{g}\sigma_j^2\mathbf{I}_{|\text{pa}(j)|}\right).\end{aligned}\quad (15)$$

In addition, to guarantee the identifiability of the DAG-probit model, we fix $\sigma_1^2 = 1$, so that instead of $p(\sigma_1^2, \mathbf{L}_{\prec 1})$ we need only to consider $p(\mathbf{L}_{\prec 1})$ with $\mathbf{L}_{\prec 1} \sim \mathcal{N}_{|\text{pa}(1)|}(\mathbf{0}, g^{-1}\mathbf{I}_{|\text{pa}(1)|})$; see also Section 2.2. Recall that (15) applies only to a complete DAG \mathcal{D} .

Consider now the case in which \mathcal{D} is not complete. The idea is to leverage (15) to construct a prior on (\mathbf{D}, \mathbf{L}) , the Cholesky parameters of $\mathbf{\Omega} \in \mathcal{P}_{\mathcal{D}}$, which is valid for *any* \mathcal{D} . To this end we follow the procedure of [Geiger & Heckerman \(2002\)](#). Specifically, let \mathcal{D} be an arbitrary DAG and assume a parent ordering of its nodes. For each node $j \in \{1, \dots, q\}$, let $\{\sigma_j^2, \mathbf{L}_{\prec j}\}$ be the Cholesky parameters associated to node j , and identify a *complete* DAG $\mathcal{D}^{C(j)}$ such that $\text{pa}_{\mathcal{D}^{C(j)}}(j') = \text{pa}_{\mathcal{D}}(j)$, where j' in $\mathcal{D}^{C(j)}$ corresponds to the same variable as j in \mathcal{D} . Because of the parent ordering $j' = q - |\text{pa}_{\mathcal{D}}(j)|$ which is usually different from j . Let $\{\sigma_{j'}^{2C(j)}, \mathbf{L}_{\prec j'}^{C(j)}\}$ be the Cholesky parameters of node j' under the complete DAG $\mathcal{D}^{C(j)}$. We then assign to $\{\sigma_j^2, \mathbf{L}_{\prec j}\}$ the same prior of $\{\sigma_{j'}^{2C(j)}, \mathbf{L}_{\prec j'}^{C(j)}\}$ which can be gathered from Equation (15) in the complete DAG-Wishart version. In particular $\sigma_j^2 \sim \text{I-Ga}((a + |\text{pa}_{\mathcal{D}}(j)| - q + 3)/2 - 1, g/2)$ and $\mathbf{L}_{\prec j}$ is distributed as a zero-mean multivariate normal with covariance matrix $g^{-1}\sigma_j^2\mathbf{I}_{|\text{pa}_{\mathcal{D}}(j)|}$. Therefore both distributions only depend on the cardinality of $\text{pa}_{\mathcal{D}}(j)$ which is the same across alternative parent orderings. Finally, by assuming independence among node-parameters $(\sigma_j^2, \mathbf{L}_{\prec j})$, we can write

$$p(\mathbf{D}, \mathbf{L}) = \prod_{j=1}^q p(\sigma_j^2, \mathbf{L}_{\prec j}), \quad (\mathbf{L}, \mathbf{D}) \in \Theta_{\mathcal{D}}, \quad (16)$$

where $\Theta_{\mathcal{D}}$ is the image of the space $\mathcal{P}_{\mathcal{D}}$ under the mapping $\mathbf{\Omega} \mapsto (\mathbf{D}, \mathbf{L})$.

4.2 Prior on DAG space

For a given DAG \mathcal{D} , let $\mathbf{A}^{\mathcal{D}}$ be the (symmetric) 0-1 adjacency matrix of the skeleton of \mathcal{D} whose (u, v) element is denoted by $\mathbf{A}_{(u,v)}^{\mathcal{D}}$. Conditionally on the edge inclusion probability π , we first assign a Bernoulli prior independently to each element $\mathbf{A}_{(u,v)}^{\mathcal{D}}$ belonging to the lower-triangular part, that is: $\mathbf{A}_{(u,v)}^{\mathcal{D}} \mid \pi \stackrel{iid}{\sim} \text{Ber}(\pi), u > v$. As a consequence we get

$$p(\mathbf{A}^{\mathcal{D}}) = \pi^{|\mathbf{A}^{\mathcal{D}}|} (1 - \pi)^{\frac{q(q-1)}{2} - |\mathbf{A}^{\mathcal{D}}|}, \quad (17)$$

where $|\mathbf{A}^{\mathcal{D}}|$ denotes the number of edges in the skeleton, equivalently the number of entries equal to one in the lower-triangular part of $\mathbf{A}^{\mathcal{D}}$. Finally, we set $p(\mathcal{D}) \propto p(\mathbf{A}^{\mathcal{D}})$, for $\mathcal{D} \in \mathcal{S}_q$, where \mathcal{S}_q is the set of all DAGs on q nodes.

4.3 Posterior distribution of θ_0

As mentioned, in absence of substantive prior information, we assign a flat improper prior to the threshold $\theta_0 \in (-\infty, \infty)$, $p(\theta_0) \propto 1$. Accordingly, we need to prove that the posterior of θ_0 is proper. The next proposition details under which conditions 2 is guaranteed.

Proposition 4.1. *Under the prior (15) for (\mathbf{D}, \mathbf{L}) , $p(\mathcal{D})$ as in Section 4.2 for DAG \mathcal{D} and the improper prior $p(\theta_0) \propto 1$ for θ_0 , the posterior of θ_0 is proper provided the sample contains at least two observations with distinct values for Y , that is $y_i = 1, y_{i'} = 0$ ($i \neq i'$).*

Proof. See Supplementary material (Castelletti & Consonni, 2020b). □

Additionally, we prove in the Supplementary material that under the conditions of Proposition 4.1 the joint posterior of $(\mathbf{D}, \mathbf{L}, \mathcal{D}, \theta_0, \mathbf{X}_1)$ is proper. Clearly, alternative priors for θ_0 might have been used; yet the full conditional of θ_0 would not be amenable to direct sampling. As a consequence, posterior inference on θ_0 is performed through a Metropolis Hastings step inside our MCMC scheme; see Section 5 for details.

5 MCMC scheme

In this section we detail the MCMC scheme that we adopt to target the posterior distribution

$$p(\mathbf{D}, \mathbf{L}, \mathcal{D}, \theta_0, \mathbf{X}_1 \mid \mathbf{y}, \mathbf{X}_{-1}) \propto f(\mathbf{y}, \mathbf{X} \mid \mathbf{D}, \mathbf{L}, \mathcal{D}, \theta_0) p(\mathbf{D}, \mathbf{L} \mid \mathcal{D}) p(\mathcal{D}), \quad (18)$$

now emphasizing the dependence on DAG \mathcal{D} , where $\mathbf{X}_{-1} = (\mathbf{X}_2, \dots, \mathbf{X}_q)$, and the term $p(\theta_0)$ has been omitted because it is proportional to one.

5.1 Update of (D, L, \mathcal{D})

From (18) the full conditional distribution of (D, L, \mathcal{D}) is

$$p(D, L, \mathcal{D} | \mathbf{y}, \mathbf{X}, \theta_0) \propto p(\mathbf{X} | D, L, \mathcal{D}) p(D, L | \mathcal{D}) p(\mathcal{D})$$

using (9), where $\mathbf{X} = (\mathbf{X}_1, \mathbf{X}_2, \dots, \mathbf{X}_q)$ is the (n, q) augmented data matrix.

To sample from $p(D, L, \mathcal{D} | \mathbf{X})$ we adopt a reversible jump MCMC algorithm which takes into account the partial analytic structure (PAS, [Godsill 2012](#)) of the DAG-Wishart distribution to sample DAG \mathcal{D} and the Cholesky parameters (D, L) from their full conditional. A similar approach was implemented in [Wang & Li \(2012\)](#) for Gaussian undirected graphical models using G-Wishart priors. Details about the PAS algorithm and its implementation in our DAG setting are reported in the Supplementary material ([Castelletti & Consonni, 2020b](#)).

Specifically, at each iteration of the MCMC scheme, we first propose a new DAG \mathcal{D}' from a suitable proposal distribution $q(\mathcal{D}' | \mathcal{D})$; see again our Supplementary material. In particular, it is shown that when proposing a DAG \mathcal{D}' which differs from the current graph \mathcal{D} by one edge (h, j) , the acceptance probability for \mathcal{D}' is given by

$$\alpha_{\mathcal{D}'} = \min \left\{ 1, \frac{m(\mathbf{X}_j | \mathbf{X}_{\text{pa}_{\mathcal{D}'}(j)}, \mathcal{D}')}{m(\mathbf{X}_j | \mathbf{X}_{\text{pa}_{\mathcal{D}}(j)}, \mathcal{D})} \cdot \frac{p(\mathcal{D}')}{p(\mathcal{D})} \cdot \frac{q(\mathcal{D} | \mathcal{D}')}{q(\mathcal{D}' | \mathcal{D})} \right\} \quad (19)$$

where, for $j \in \{2, \dots, q\}$,

$$m(\mathbf{X}_j | \mathbf{X}_{\text{pa}_{\mathcal{D}}(j)}, \mathcal{D}) = (2\pi)^{-\frac{n}{2}} \frac{|\mathbf{T}_j|^{1/2}}{|\bar{\mathbf{T}}_j|^{1/2}} \cdot \frac{\Gamma(a_j^* + \frac{n}{2})}{\Gamma(a_j^*)} \left[\frac{1}{2}g \right]^{a_j^*} \left[\frac{1}{2}(g + \mathbf{X}_j^\top \mathbf{X}_j - \hat{\mathbf{L}}_j^\top \bar{\mathbf{T}}_j \hat{\mathbf{L}}_j) \right]^{-(a_j^* + n/2)} \quad (20)$$

with

$$\begin{aligned} \mathbf{T}_j &= g\mathbf{I}_{|\text{pa}_{\mathcal{D}}(j)|} \\ \bar{\mathbf{T}}_j &= g\mathbf{I}_{|\text{pa}_{\mathcal{D}}(j)|} + \mathbf{X}_{\text{pa}_{\mathcal{D}}(j)}^\top \mathbf{X}_{\text{pa}_{\mathcal{D}}(j)} \\ \hat{\mathbf{L}}_j &= (g\mathbf{I}_{|\text{pa}_{\mathcal{D}}(j)|} + \mathbf{X}_{\text{pa}_{\mathcal{D}}(j)}^\top \mathbf{X}_{\text{pa}_{\mathcal{D}}(j)})^{-1} \mathbf{X}_{\text{pa}_{\mathcal{D}}(j)}^\top \mathbf{X}_j, \end{aligned}$$

$a_j^* = \frac{a_j}{2} - \frac{|\text{pa}_{\mathcal{D}}(j)|}{2} - 1$ and $\mathbf{X}_{\text{pa}_{\mathcal{D}}(j)}$ denotes the $(n, |\text{pa}_{\mathcal{D}}(j)|)$ sub-matrix of \mathbf{X} whose columns belong to the set $\text{pa}_{\mathcal{D}}(j)$. For $j = 1$, because we fixed $\sigma_1^2 = 1$, we have instead

$$m(\mathbf{X}_1 | \mathbf{X}_{\text{pa}_{\mathcal{D}}(1)}, \mathcal{D}) = (2\pi)^{-\frac{n}{2}} \frac{|\mathbf{T}_1|^{1/2}}{|\bar{\mathbf{T}}_1|^{1/2}} \cdot \exp \left\{ -\frac{1}{2}(\mathbf{X}_1^\top \mathbf{X}_1 + \hat{\mathbf{L}}_1^\top \bar{\mathbf{T}}_1 \hat{\mathbf{L}}_1) \right\}, \quad (21)$$

with $\mathbf{T}_1, \bar{\mathbf{T}}_1, \hat{\mathbf{L}}_1$ defined in analogy with the expressions appearing after (20); see the Supplementary material ([Castelletti & Consonni, 2020b](#)) for details. Moreover, given DAG \mathcal{D} and \mathbf{X}_1 , the full conditional of (D, L) reduces to the augmented posterior $p(D, L | \mathbf{X})$, which is conditional

on the actual data $(\mathbf{X}_2, \dots, \mathbf{X}_q)$ as well as the latent values \mathbf{X}_1 and can be easily sampled from. Specifically, since

$$f(\mathbf{X} | \mathbf{D}, \mathbf{L}) = \prod_{j=1}^q d\mathcal{N}_n(\mathbf{X}_j | -\mathbf{X}_{\text{pa}_{\mathcal{D}}(j)} \mathbf{L}_{\prec j}, \sigma_j^2 \mathbf{I}_n) \quad (22)$$

and because of (16) and conjugacy of the Normal-Inverse-Gamma prior in (15) with the Normal density, the posterior distribution of the Cholesky parameters given \mathbf{X} is, for $j = 2, \dots, q$,

$$\begin{aligned} \sigma_j^2 | \mathbf{X} &\sim \text{I-Ga} \left(a_j^* + \frac{n}{2}, \frac{1}{2} (g + \mathbf{X}_j^\top \mathbf{X}_j - \hat{\mathbf{L}}_j^\top \bar{\mathbf{T}}_j \hat{\mathbf{L}}_j) \right), \\ \mathbf{L}_{\prec j} | \sigma_j^2, \mathbf{X} &\sim \mathcal{N}_{|\text{pa}_{\mathcal{D}}(j)|}(-\hat{\mathbf{L}}_j, \sigma_j^2 \bar{\mathbf{T}}_j^{-1}). \end{aligned} \quad (23)$$

Moreover, for node 1 where $\sigma_1^2 = 1$, we have

$$\mathbf{L}_{\prec 1} | \mathbf{X} \sim \mathcal{N}_{|\text{pa}_{\mathcal{D}}(1)|}(-\hat{\mathbf{L}}_1, \bar{\mathbf{T}}_1^{-1}). \quad (24)$$

5.2 Update of \mathbf{X}_1 and θ_0

Updating of $\mathbf{X}_1 = (x_{1,1}, \dots, x_{n,1})^\top$ can be performed by direct sampling from the full conditional distribution of each latent observation $x_{i,1}$,

$$f(x_{i,1} | y_i, x_{i,2}, \dots, x_{i,q}, \mathbf{D}, \mathbf{L}, \mathcal{D}, \theta_0) \propto f(x_{i,1} | \mathbf{x}_{i,\text{pa}_{\mathcal{D}}(1)}, \mathbf{L}_{\prec j}) \cdot \mathbb{1}(\theta_{y_i-1} < x_{i,1} \leq \theta_{y_i}),$$

which corresponds to a $\mathcal{N}(-\mathbf{L}_{\prec 1}^\top \mathbf{x}_{i,\text{pa}_{\mathcal{D}}(1)}, 1)$ truncated at the interval $(\theta_{y_i-1}, \theta_{y_i}]$.

Finally, the cut-off θ_0 is updated through a Metropolis Hastings step where, given the current value θ_0 , a candidate value g_0 is proposed from $q(g_0 | \theta_0) = d\mathcal{N}(g_0 | \theta_0, \sigma_0^2)$. We then set $\theta_0 = g_0$ with probability

$$\alpha_\theta = \min \{1; r_\theta\}, \quad (25)$$

where

$$r_\theta = \frac{\prod_{i=1}^n \left[\Phi(g_{y_i} | -\mathbf{L}_{\prec 1}^\top \mathbf{x}_{i,\text{pa}_{\mathcal{D}}(1)}, 1) - \Phi(g_{y_i-1} | -\mathbf{L}_{\prec 1}^\top \mathbf{x}_{i,\text{pa}_{\mathcal{D}}(1)}, 1) \right]}{\prod_{i=1}^n \left[\Phi(\theta_{y_i} | -\mathbf{L}_{\prec 1}^\top \mathbf{x}_{i,\text{pa}_{\mathcal{D}}(1)}, 1) - \Phi(\theta_{y_i-1} | -\mathbf{L}_{\prec 1}^\top \mathbf{x}_{i,\text{pa}_{\mathcal{D}}(1)}, 1) \right]} \cdot \frac{d\mathcal{N}(\theta_0 | g_0, \sigma_0^2)}{d\mathcal{N}(g_0 | \theta_0, \sigma_0^2)},$$

and $g_{-1} = \infty, g_1 = +\infty$.

5.3 Algorithm

Algorithm 1 summarizes our MCMC scheme. The output is a collection of DAGs $\{\mathcal{D}^{(t)}\}_{t=1}^T$ and Cholesky parameters $\{(\mathbf{D}^{(t)}, \mathbf{L}^{(t)})\}_{t=1}^T$ approximatively sampled from the target distribution (18). In particular we can compute posterior summaries of interest such as the posterior probabilities of edge inclusion, namely

$$\hat{p}_{u \rightarrow v}(\mathbf{y}, \mathbf{X}_2, \dots, \mathbf{X}_q) \equiv \hat{p}_{u \rightarrow v} = \frac{1}{T} \sum_{t=1}^T \mathbb{1}_{u \rightarrow v} \{\mathcal{D}^{(t)}\}, \quad (26)$$

where $\mathbb{1}_{u \rightarrow v} \{\mathcal{D}^{(t)}\}$ takes value 1 if and only if $\mathcal{D}^{(t)}$ contains the edge $u \rightarrow v$. Moreover, we can reconstruct the covariance matrices $\{\Sigma^{\mathcal{D}^{(t)}}\}_{t=1}^T$ using (5). The latter can be subsequently retrieved to obtain for selected $s \in \{2, \dots, q\}$ and intervention value \tilde{x} the collection of causal effects $\{\beta_s^{(t)}(\tilde{x})\}_{t=1}^T$ defined in (13), where we set $\beta_s^{(t)}(\tilde{x}) \equiv \beta_s(\tilde{x}, \Sigma^{\mathcal{D}^{(t)}}, \theta_0^{(t)})$. An overall summary of the causal effect of $\text{do}(X_s = \tilde{x})$ on Y can be computed as

$$\hat{\beta}_s^{BMA}(\tilde{x}) = \frac{1}{T} \sum_{t=1}^T \beta_s^{(t)}(\tilde{x}), \quad (27)$$

which corresponds to a Bayesian Model Averaging (BMA) estimate where posterior (DAG) model probabilities are approximated through the MCMC frequencies of visits; see [García-Donato & Martínez-Beneito \(2013\)](#) for a discussion of the merits of frequency based estimators in large model spaces.

Algorithm 1: MCMC scheme to sample from (18)

Input: A dataset $(\mathbf{y}, \mathbf{X}_2, \dots, \mathbf{X}_q)$

Output: T samples from the posterior (18)

- 1 Initialize $\mathcal{D}^{(0)}$, e.g. the empty DAG, the cut-offs $\theta_{-1}^{(0)} = -\infty, \theta_0^{(0)} = 0, \theta_1^{(0)} = +\infty$ and the latent variables $\mathbf{x}_1^{(0)}$, e.g. $x_{i,1}^{(0)} \stackrel{\text{ind}}{\sim} \mathcal{N}(0, 1)$ truncated at $(\theta_{y_i-1}^{(0)}, \theta_{y_i}^{(0)})$;
 - 2 **for** $t = 1, \dots, T$ **do**
 - 3 Sample \mathcal{D}' from $q(\mathcal{D}' | \mathcal{D}^{(t-1)})$ and set $\mathcal{D}^{(t)} = \mathcal{D}'$ with probability $\alpha_{\mathcal{D}}$ (19), otherwise $\mathcal{D}^{(t)} = \mathcal{D}^{(t-1)}$;
 - 4 Sample $(\mathbf{D}^{\mathcal{D}^{(t)}}, \mathbf{L}^{\mathcal{D}^{(t)}})$ from its augmented posterior distribution (23);
 - 5 For $i = 1, \dots, n$, independently sample $x_{i,1}$ from $\mathcal{N}(-\mathbf{L}_{\prec 1}^{\mathcal{D}^{(t)\top}} \mathbf{x}_{i, \text{pa}_{\mathcal{D}^{(t)}}(1)}, 1)$ truncated at $(\theta_{y_i-1}^{(t)}, \theta_{y_i}^{(t)})$;
 - 6 Propose a cut-off g_0 from $q(g_0 | \theta_0^{(t)})$ and set $\theta_0^{(t)} = g_0$ with probability α_{θ} (25), otherwise $\theta_0^{(t)} = \theta_0^{(t-1)}$; set $\theta_{-1}^{(t)} = -\infty, \theta_1^{(t)} = +\infty$.
 - 7 **end**
-

6 Simulations

In this section we evaluate the performance of our method through simulation studies. Specifically, for each combination of number of nodes $q \in \{20, 40\}$ and sample size $n \in \{100, 200, 500\}$, which we call simulation *scenario*, we generate 40 DAGs using a probability of edge inclusion equal to $p = 3/(2q - 2)$ to induce sparsity; see [Peters & Bühlmann \(2014\)](#). For each DAG \mathcal{D} we then proceed as follows. We identify a parent ordering and fix $\mathbf{D}^{\mathcal{D}} = \mathbf{I}_q$ and then randomly sample the entries of $\mathbf{L}^{\mathcal{D}}$ in the interval $[-2, -1] \cup [1, 2]$; next we generate a dataset consisting of n i.i.d. q -dimensional observations from the structural equation model (4) which also includes

the $(n, 1)$ vector of latent observations; we finally fix the threshold $\theta_0 = 0$ and obtain the 0-1 vector of responses $\mathbf{y} = (y_1, \dots, y_n)^\top$ as in (7).

We apply Algorithm 1 to approximate the target distribution in (18) by setting the number of MCMC iterations $T = 25000$ for $q = 20$, and $T = 50000$ for $q = 40$. We also set $g = 1/n$ and $a = q + 1$ in the prior on the Cholesky parameters of $\mathbf{\Omega}$ (15) and $\sigma_0^2 = 0.25$ in the proposal density for the cut-off θ_0 .

We begin by evaluating the global performance of our method in learning the graph structure. To this end, we first estimate the posterior probabilities of edge inclusion by computing $\hat{p}_{u \rightarrow v}(\cdot)$ in (26) for each pair of distinct nodes u, v . Next, we consider a threshold for edge inclusion $k \in [0, 1]$ and for a given k construct a DAG estimate by including those edges (u, v) whose posterior probability exceeds k . The resulting graph is compared with the true DAG through the sensitivity (SEN) and specificity (SPE) indexes, respectively defined as

$$SEN = \frac{TP}{TP + FN}, \quad SPE = \frac{TN}{TN + FP},$$

where TP, TN, FP, FN are the numbers of true positives, true negatives, false positives and false negatives respectively. The two indexes are used to construct a receiver operating characteristic (ROC) curve. Specifically, for each scenario defined by q and n , we present a ROC curve constructed as follows. For each threshold k , we compute SEN and $(1 - SPE)$ under each of the 40 DAGs used in the simulation. The point whose coordinates are the mean of each of the two measures corresponds to one dot in Figure 1. The collection of dots connected by lines represents an average ROC curve. We proceed similarly to compute the 5th and 95th percentile and obtain the grey band.

To better appreciate Figure 1, we also compute, for each simulation scenario (q, n) , the area under the (average) ROC curve (AUC) whose values are reported in Table 1. They are close or above 94% under the three sample sizes considered when $q = 20$. When $q = 40$ AUC exceeds 90% for $n = 100$ and rises to over 97% for $n = 500$.

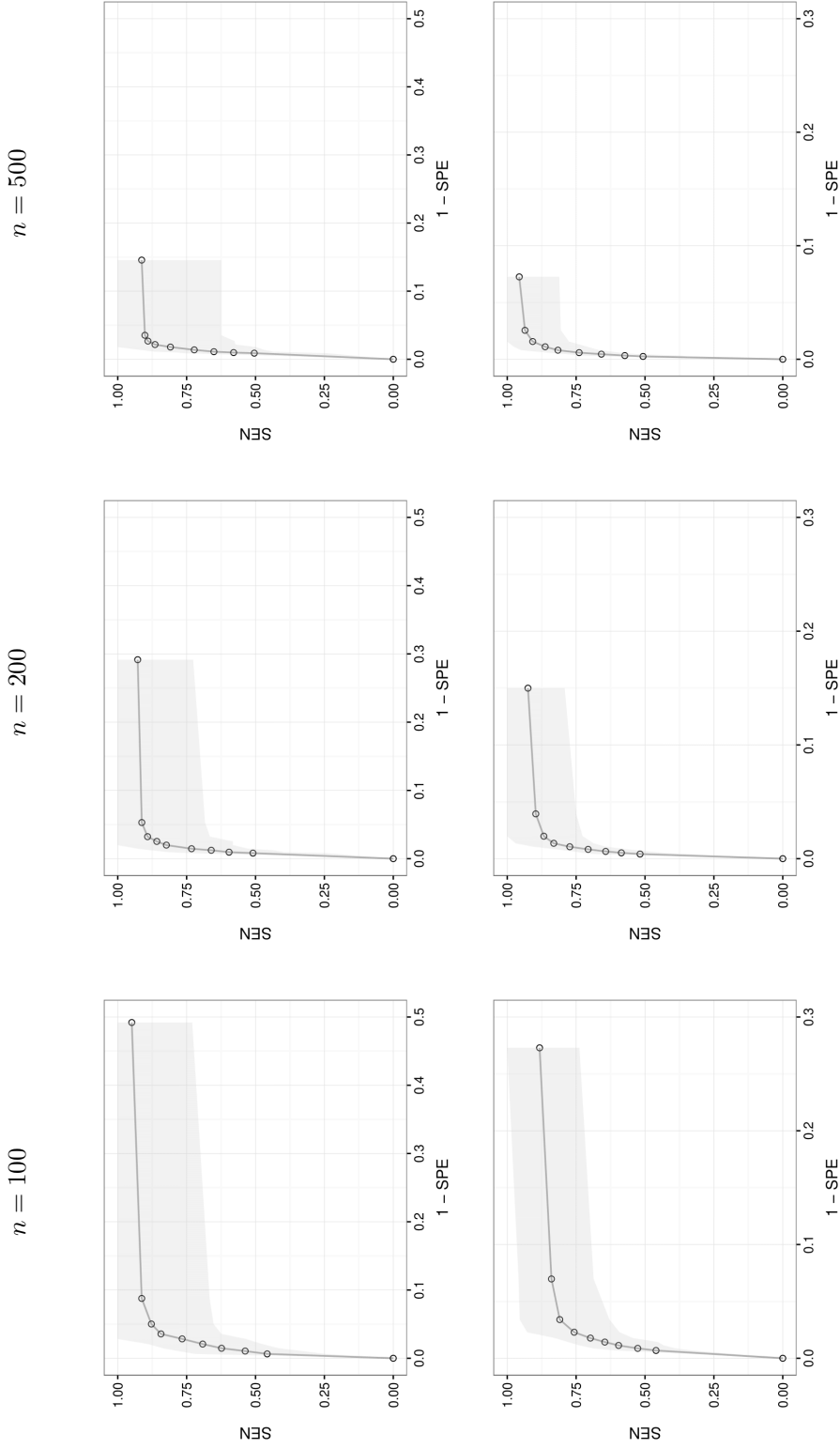


Figure 1: Simulations. Receiver operating characteristic (ROC) curve obtained under varying thresholds for the posterior probabilities of edge inclusion for each combination of number of nodes $q = \{20, 40\}$ (first and second row respectively) and sample size $n \in \{100, 200, 500\}$. Dots and connecting line describe the (average over the 40 simulated DAGs) ROC curve, while the grey area represents the 5th-95th percentile band.

	$n = 100$	$n = 200$	$n = 500$
$q = 20$	93.89	94.19	95.12
$q = 40$	90.94	94.91	97.19

Table 1: Simulations. Area under the curve (percentage values) computed from the average ROC curves in Figure 1 for number of nodes $q \in \{20, 40\}$ and sample sizes $n \in \{100, 200, 500\}$.

A more specific check on the ability of our method in recovering the structure of the underlying DAG can be considered. Since Y is the response, interest centers on the causal effect on Y following an intervention on a variable in the system. A natural group of intervention variables is represented by the set of parents of the latent node X_1 either because they directly influence X_1 (and hence Y) or because they act as intermediate nodes along a pathway originating from a variable upstream in the graph. To this end, under each simulation scenario, we fix the threshold for edge inclusion $k^* = 0.5$ and include those edges $u \rightarrow 1$ such that $\hat{p}_{u \rightarrow 1}(\cdot) \geq 0.5$ in analogy with the median probability model of Barbieri & Berger (2004). The resulting 0-1 vector of indicators for edge inclusion is $\mathbf{a} = (a_{1,1}, \dots, a_{q,1})^\top$, where $a_{1,1} = 0$ while, for $u = 2, \dots, q$, $a_{u,1} = 1$ if $u \rightarrow 1$ is included, 0 otherwise. Next we compute the proportion of predictors that are correctly classified,

$$p^* = \frac{1}{q-1} \sum_{u=2}^q \mathbb{I}\{a_{u,1} = \mathbf{A}_{(u,1)}^{\mathcal{D}}\},$$

where $\mathbf{A}_{(u,v)}^{\mathcal{D}}$ denotes the (u, v) element of the adjacency matrix of \mathcal{D} . The results are summarized in the box-plots of Figure 2 where we report the frequency distribution of p^* computed over the 40 true DAGs. While for $n = 100$ the proportion of correctly classified edges presents some variability with a median which is nevertheless around 80% ($q = 40$) and 90% ($q = 20$), the performance greatly improves as the sample size increases with practically all values being close to 1.

We now focus on causal effect estimation. Under each simulated DAG \mathcal{D} and parameters $(\mathbf{D}^{\mathcal{D}}, \mathbf{L}^{\mathcal{D}})$ we first compute the (true) covariance matrix $\Sigma^{\mathcal{D}}$ using (5). Now recall from (13) that the causal effect on Y is a probability which also depends on the level \tilde{x} assigned to the intervened variable X_s . For each intervened node $s \in \{2, \dots, q\}$ we evaluate $\beta_s(\tilde{x}, \Sigma^{\mathcal{D}}, \theta_0) \equiv \beta_s^{\text{true}}(\tilde{x})$ at each observed value of X_s in the simulation scenario, $(x_{1,s}, \dots, x_{n,s})$, and obtain the $(n, 1)$ vector of causal effects $(\beta_s^{\text{true}}(x_{1,s}), \dots, \beta_s^{\text{true}}(x_{n,s}))^\top$. Next we produce the collection of BMA estimates $\hat{\beta}_s^{\text{BMA}}(x_{1,s}), \dots, \hat{\beta}_s^{\text{BMA}}(x_{n,s})$ according to Equation (27). To evaluate the performance of our method in estimating the causal effect we consider the differences $(\beta_s^{\text{true}}(x_{i,s}) - \hat{\beta}_s^{\text{BMA}}(x_{i,s}))$ and compute the mean absolute error (MAE)

$$MAE_s = \frac{1}{n} \sum_{i=1}^n |\beta_s^{\text{true}}(x_{i,s}) - \hat{\beta}_s^{\text{BMA}}(x_{i,s})|,$$

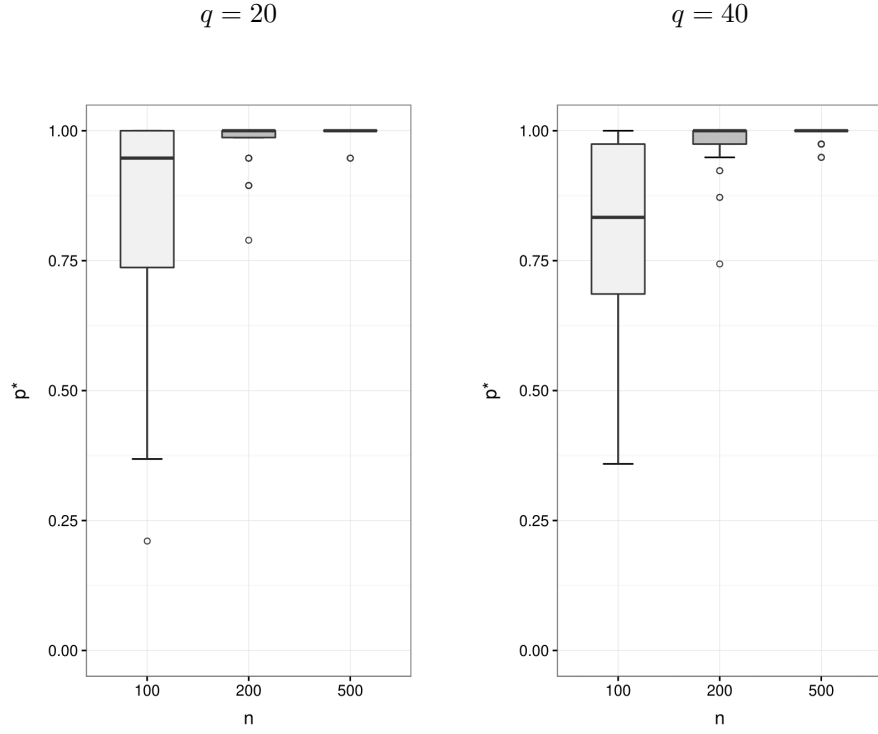


Figure 2: Simulations. Distribution across 40 simulated datasets of the proportion of predictors p^* that are correctly classified given a threshold for edge inclusion $k^* = 0.5$ for each combination of number of nodes $q \in \{20, 40\}$ and sample size $n \in \{100, 200, 500\}$.

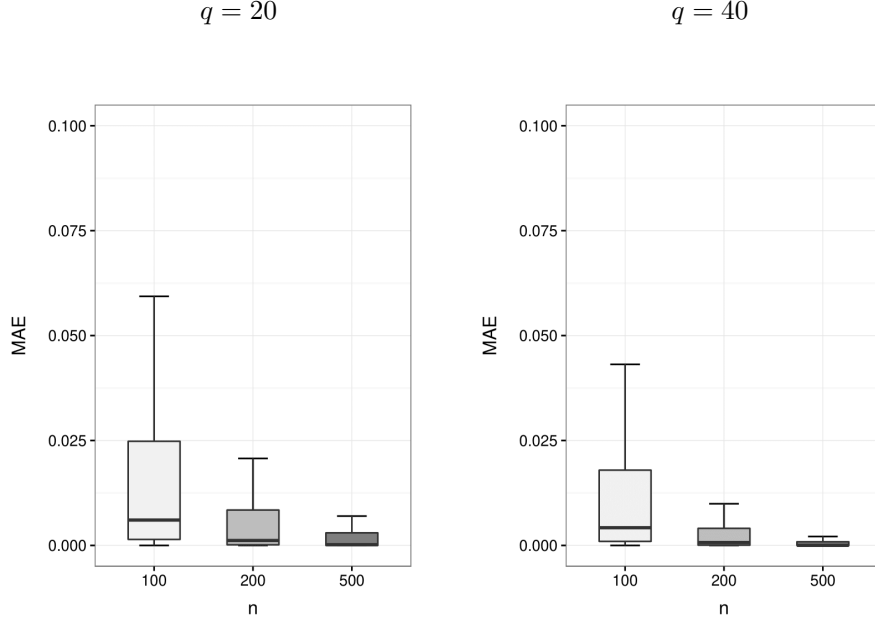


Figure 3: Simulations. Distribution over 40 datasets and nodes $s \in \{2, \dots, q\}$ of the mean absolute error (MAE) of BMA estimates of true causal effects. Results are presented for each combination of number of nodes $q \in \{20, 40\}$ and sample size $n \in \{100, 200, 500\}$.

for each intervened node $s = 2, \dots, q$. Results are summarized in the box-plots of Figure 3, where we report the distribution of the MAE (constructed across the 40 DAGs and nodes $s = 2, \dots, q$) as a function of n . As expected, MAE decreases and approaches 0 as the sample size n grows for both values of q . Notice that the median value of MAE in the worst case scenario ($q = 20, n = 100$) is about half of one percent.

Finally, we also explore settings where $n \leq q$: in particular we include simulation results for $q = 40$ and $n \in \{10, 20, 40\}$. Again, we generate 40 DAGs and the allied parameters as in our first simulation study. Results are summarized in the box-plots of Figure 4, where we report the distribution of the MAE, constructed across the 40 DAGs and nodes $s \in \{2, \dots, q\}$ as a function of n . It appears that, even if sample sizes are moderate, MAE decreases as n grows.

7 Analysis of gene expressions from breast cancer cells

In this section we apply our method to a gene expression dataset presented in Yin et al. (2014). The aim of the original study was to evaluate the ability of a gene signature derived from breast cancer stem cells to predict the risk of metastasis and survival in breast cancer patients. To this end, a collection of genes which are believed to be the main responsible for tumor

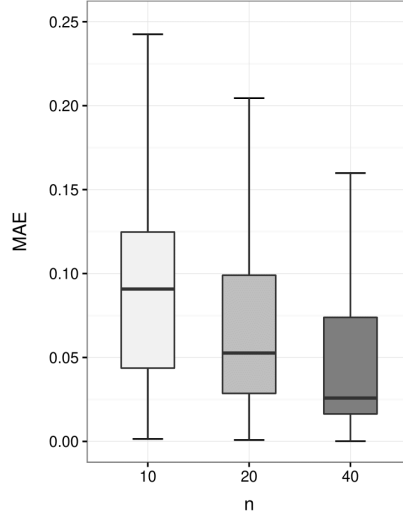


Figure 4: Simulations. Distribution over 40 datasets and nodes $s \in \{2, \dots, q\}$ of the mean absolute error (MAE) of BMA estimates of true causal effects. Results are presented for number of nodes $q = 40$ and sample size $n \in \{10, 20, 40\}$.

initiation, progression, and response to therapy was considered. The study was motivated by recent literature establishing the existence of a rare population of cells, called *stem-like cells*, which supposedly represent the cellular origin of cancer; see for instance [OBrien et al. \(2006\)](#). Gene-expression levels were measured on $n = 198$ breast cancer patients of which 62 manifested distant metastasis. In the following we consider the expression levels of $q = 28$ genes included in the original study and a binary response variable Y indicating the occurrence (absence or presence, respectively $Y = 0$ and $Y = 1$) of distant metastasis. Evaluating the causal effect on Y due to an hypothetical intervention on a specific gene which sets its expression level may help understand which genes are particularly relevant for determining distant metastasis. This in turn can be useful to identify external interventions, which are known to induce variations in the expression of specific genes. For instance epigenetic modifications of gene expressions may be induced by lifestyle and environmental factors such as nutrition-dietary components, exercise, physical activity and toxins; see [Abdul et al. \(2017\)](#). Similarly [Campbell et al. \(2017\)](#) examine the effects of lifestyle interventions on proposed biomarkers of lifestyle and cancer risk at the level of adipose tissue in humans.

We apply Algorithm 1 by fixing the number of MCMC iterations $T = 120000$. Observations from the continuous variables X_2, \dots, X_q were standardized. We also set $g = 1/n$ and $a = q + 1$ in the prior on the Cholesky parameters of Ω as in the simulation scenarios of Section 6. We first use the MCMC output to estimate the posterior probability of inclusion of each directed edge

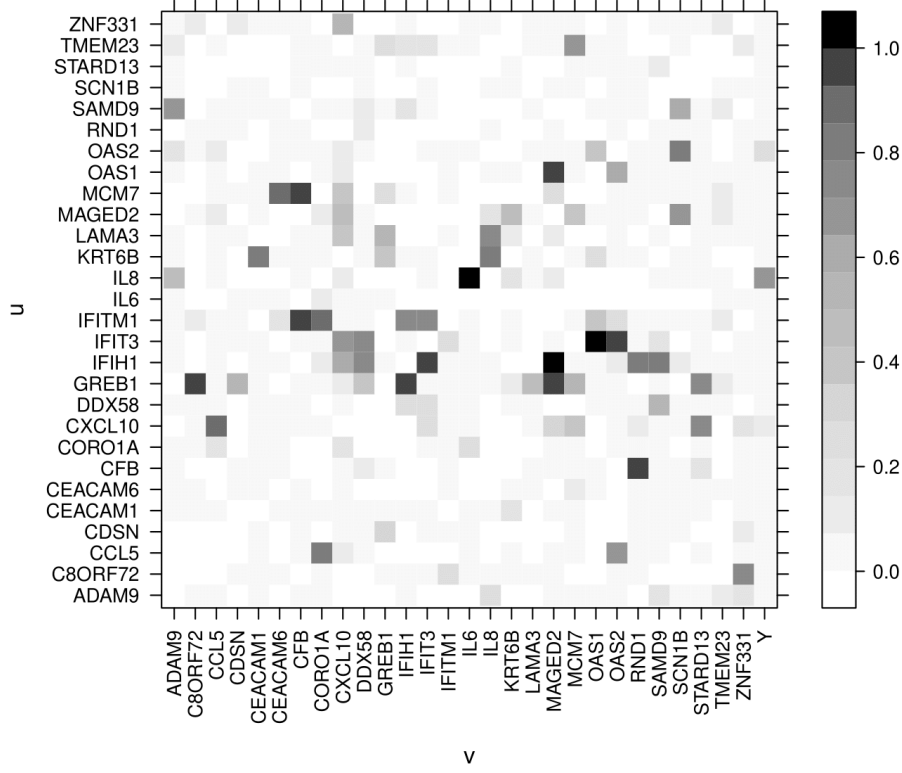


Figure 5: Gene expression data. Heat map with estimated marginal posterior probabilities of edge inclusion for each edge $u \rightarrow v$.

$u \rightarrow v$, that we report in the heat map of Figure 5. Results show a substantial degree of sparsity in the underlying graph structure and only 48 edges have a posterior probability of inclusion exceeding 0.5. Moreover, among the 28 genes, only gene IL8, for which $\hat{p}_{\text{IL8} \rightarrow Y}(\cdot) = 0.70$, seems to directly affect the response variable.

To evaluate the incidence of each gene on the probability of recurrence we compute the causal effect (13) on the response due to an intervention on a specific gene. To this end, starting from the MCMC output we produce a BMA estimate $\hat{\beta}_s^{BMA}(\tilde{x})$ for each gene $s = 2, \dots, q$ according to (27). Since the causal effect depends on the level \tilde{x} assigned to the intervened variable X_s , we evaluate $\hat{\beta}_s^{BMA}(\tilde{x})$ at each observed value of X_s , that is $x_{1,s}, \dots, x_{n,s}$. The results are reported in Figure 6, where each box-plot refers to a gene $s \in \{2, \dots, q\}$ and summarizes the distribution of $n = 198$ BMA estimates, $\{\hat{\beta}_s^{BMA}(x_{i,s})\}_{i=1}^n$. Because the data were standardized, the ranges of X_2, \dots, X_q are similar and we can meaningfully compare results across genes.

Recall from Proposition 3.1 that γ_s is the covariance between X_s and X_1 . If $\gamma_s = 0$, Equation (13) shows that the causal effect on Y due to an intervention on X_s does not vary with \tilde{x} . If

prior information is weak in relation to the sample size, the estimate of the causal effect will be close to the overall frequency of distant metastasis in the sample (0.31). This is the situation exhibited by most genes in Figure 6. On the other hand if γ_s is not zero, the collection of causal effects evaluated at x_{is} , $i = 1, \dots, n$ will vary. Since the observations are centred, their average is zero and the causal effects will be spread around the value corresponding to the average $\bar{x}_s = 0$ whose estimate is 0.31 as indicated above. This is what happens for a few genes such as IL8, OAS2 and KRT6B, which exhibit a much greater variability of the causal effect across their measurements, implying that their regulation can influence the occurrence of distant metastasis. In particular, gene IL8 has also been identified as having a potential impact on cancer cells in several studies (Waugh & Wilson, 2008). Other genes which stand out in terms of variability are OAS2 and KRT6B, with the latter not directly linked to Y (as one can see from the heat map of Figure 5) and exhibiting a moderate causal effect on Y which is likely due to the strong association of KRT6B with IL8 (as it emerges from the posterior probabilities of edge inclusion in Figure 5).

For genes IL8 and OAS2 we also report in Figure 7 more detailed results for causal effect estimation. In particular, each plot reports the BMA estimates $\{\hat{\beta}_s^{BMA}(x_{i,s})\}_{i=1}^n$ (represented by $n = 198$ dots), and the corresponding credible regions at level 95% represented by the grey area. Results show that increasing expression levels of IL8 are likely to increase the presence of distant metastasis, with BMA estimates of the probability of recurrence ranging in the interval $[0.18; 0.54]$. This is consistent with results we have obtained showing that most of the mass of the distribution of the coefficient γ_s for these genes is assigned to the positive half-line; see also the discussion after (13). Moreover, more extreme levels of IL8 are associated with larger credible regions. A similar behavior, although less pronounced, is observed for gene OAS2 with BMA estimates ranging between $[0.25; 0.41]$.

8 Discussion

In this paper we deal with causal effect estimation from observational data. We consider a system of real-valued variables together with a binary response; interest lies in the evaluation of the causal effect on the response due to an external intervention on a variable. We assume that the response is generated by standard thresholding applied to a continuous latent variable, and assume that the joint distribution of all continuous variables belongs to a zero-mean Gaussian Directed Acyclic Graph (DAG) model, or equivalently a Structural Equation Model (SEM), and name the resulting model *DAG-probit*.

Rather than constructing a prior distribution on the covariance (or precision) matrix constrained by a given DAG, we proceed by assigning to the corresponding Cholesky parameters a DAG-Wishart prior whose hyperparameters are deduced from a single unique Wishart distri-

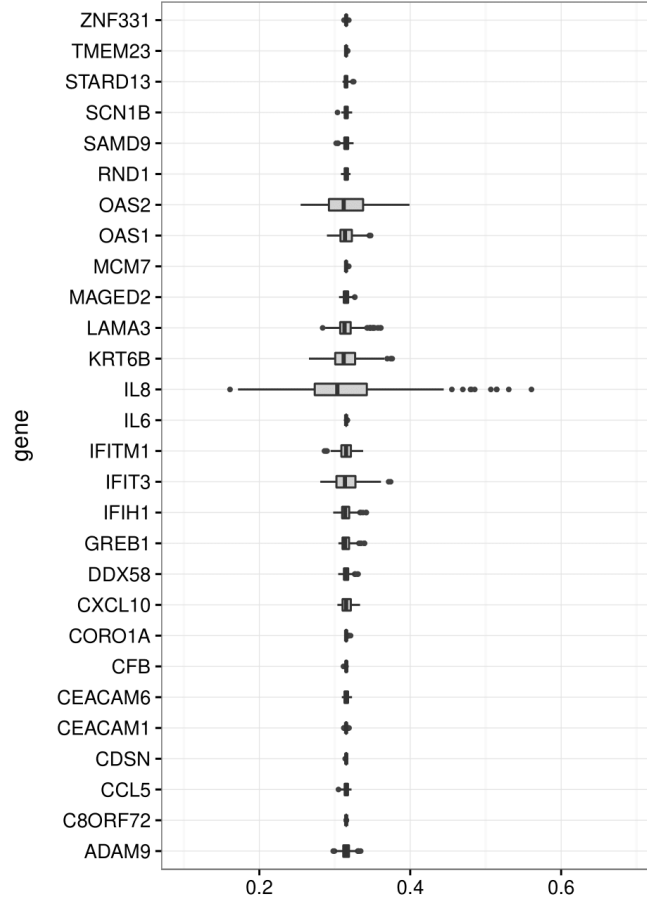


Figure 6: Gene expression data. Box-plots of BMA estimate of causal effect. Each box-plot refers to one of the 28 genes s , and represents the $n = 198$ BMA estimates computed at each observed value $(x_{1,s}, \dots, x_{n,s})$ of expression for gene s .

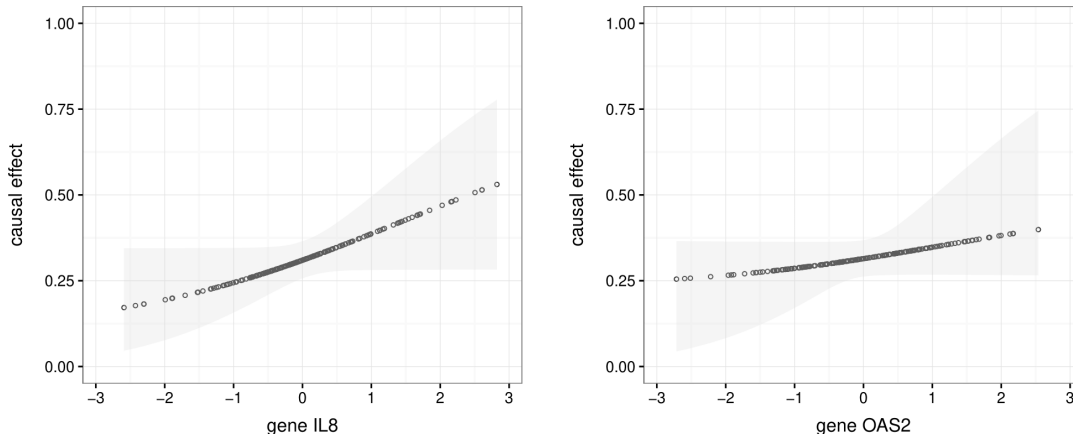


Figure 7: Gene expression data. BMA estimates (dots) and credible regions at level 95% (grey area) for two selected genes, IL8 and OAS2.

bution. This technique not only drastically simplifies prior elicitation, but has the important advantage of producing score equivalence, meaning that marginal likelihoods of Markov equivalent DAG models are all equal (Geiger & Heckerman, 2002). This feature will have a useful implication, as we discuss at the end of this section.

Because the structure of the data-generating DAG is unknown, we construct an MCMC sampler whose target is the joint posterior distribution of the DAG and the allied Cholesky parameters. This is achieved by carefully tailoring a Partial Analytic Structure (PAS) algorithm to our DAG setting. As a by-product, we recover the MCMC sequence of causal effects corresponding to each visited DAG; this represents the input to our final Bayesian Model Averaging (BMA) estimate, which naturally accounts for model uncertainty on the underlying graph structure.

The assumption of jointly normally distributed random variables can be a source of concern whenever one faces a concrete data analysis. With regard to our application the Gaussian assumption has been often used to analyse gene expression data; see for instance Dobra et al. (2004) and Markowitz & Spang (2007). In addition, it allows to easily incorporate the binary outcome through a latent component, and results in an efficient algorithm, because of closed-form expressions both for the posterior distribution of parameters, as well as for the marginal likelihood of models.

Besides the assumption of normality, our model posits a unique graphical structure as the generating mechanism of all observations. Nevertheless, some problems may suggest to partition the units into groups each having a specific graphical structure which can be however related to the other ones, as in gene expressions collected on multiple tissues from the same individual (Xie et al., 2017). In this setting a multiple graphical model setup would be more appropriate to

encourage similarities between group graphical structures; see for instance [Peterson et al. \(2015\)](#) for a Bayesian analysis of multiple Gaussian undirected graphical models. The latter could be a useful starting point for an extension of our DAG-probit model to multiple groups.

In this work we consider causal effects as obtained from interventions on single nodes. However in practice an exogenous intervention may affect many variables (genes) simultaneously and accordingly one may want to predict for instance the effect of a double or triple gene knockout on the response. Causal effect estimation from joint interventions is carried out in a Gaussian setting by [Nandy et al. \(2017\)](#) using a frequentist approach. Their results show that the causal effect of X_s on the response in a joint intervention on a given set of variables can be still expressed as a function of the covariance matrix Markov w.r.t. \mathcal{D} . The same problem can be tackled by adopting a Bayesian methodology which combines DAG structural learning and causal effect estimation and is currently under investigation by ourselves. In addition, an extension to DAG-probit models should be feasible along the lines of this paper.

The methodology adopted in this work revolves around DAGs. However, it is known that in the Gaussian setting DAGs encoding the same conditional independencies (Markov equivalent DAGs) are not distinguishable using observational data ([Verma & Pearl, 1990](#)) and can be collected into Markov equivalence classes (MECs). Accordingly, when the goal of the analysis is structural learning (model selection) MECs represent the appropriate inferential object ([Andersson et al., 1997](#)). However, if the objective is causal effect estimation, this is no longer so, because Markov equivalent DAGs may return distinct causal effects. An inspection of [\(13\)](#) reveals the reason: a causal effect depends on the parent set of the intervened node, and this may differ among DAGs within the same MEC. Yet MECs can be exploited also for causal inference, as we now detail. In a frequentist setting, [Maathuis et al. \(2009\)](#) first estimate a MEC using the classic PC algorithm ([Spirtes et al., 2000](#)), and then provide an estimate of the causal effect under each DAG within the estimated equivalence class. Alternatively, a Bayesian methodology would first determine the posterior distribution on MEC space, and then, conditionally on a given MEC, compute the posterior of each causal effect within the class (one for each DAG). A single MEC causal effect estimate can be obtained by averaging effects across DAGs, using uniform weights on equivalent DAGs. Finally, an overall Bayesian Model Averaging (BMA) estimate can be obtained by averaging MEC-conditional estimates using posterior probabilities of MECs as weights; for details see ([Castelletti & Consonni, 2020a](#)). We remark that the above strategies require an exhaustive enumeration of all DAGs belonging to a MEC, which is not feasible even for a moderate number of nodes. Accordingly one considers only the distinct causal effects within a given MEC, because these values can be efficiently recovered ([Maathuis et al., 2009](#), Algorithm 3) even in high-dimensional settings. In this work we seemingly ignore the issue of DAG Markov equivalence, and propose a causal inference procedure which directly focuses on DAG space, rather than MEC space. However, as already remarked at the beginning of

this section, our method for parameter prior construction across DAG models guarantees score equivalence for DAGs within the same MEC. This, together with a uniform prior on DAGs within the same MEC, ensures that causal effects associated to Markov equivalent DAGs will be assigned equal weights in the resulting BMA estimate.

References

- ABDUL, Q., YU, B., CHUNG, H., JUNG, H. & J.S., C. (2017). Epigenetic modifications of gene expression by lifestyle and environment. *Archives of Pharmacal Research* 40 1219–1237. URL <https://doi.org/10.1007/s12272-017-0973-3>. 18
- ALBERT, J. H. & CHIB, S. (1993). Bayesian analysis of binary and polychotomous response data. *Journal of the American Statistical Association* 88 669–679. URL <http://www.jstor.org/stable/2290350>. 2
- ANDERSSON, S. A., MADIGAN, D. & PERLMAN, M. D. (1997). A characterization of Markov equivalence classes for acyclic digraphs. *The Annals of Statistics* 25 505–541. URL <http://dx.doi.org/10.1214/aos/1031833662>. 23
- BARBIERI, M. M. & BERGER, J. O. (2004). Optimal predictive model selection. *The Annals of Statistics* 32 870–897. URL <https://doi.org/10.1214/009053604000000238>. 15
- BEN-DAVID, E., LI, T., MASSAM, H. & RAJARATNAM, B. (2015). High dimensional Bayesian inference for Gaussian directed acyclic graph models. *arXiv pre-print* URL <https://arxiv.org/abs/1109.4371>. 8
- CAMPBELL, K. L., LANDELLS, C. E., FAN, J. & BRENNER, D. R. (2017). A systematic review of the effect of lifestyle interventions on adipose tissue gene expression: Implications for carcinogenesis. *Obesity* 25 S40–S51. URL <https://onlinelibrary.wiley.com/doi/abs/10.1002/oby.22010>. 18
- CAO, X., KHARE, K. & GHOSH, M. (2019). Posterior graph selection and estimation consistency for high-dimensional Bayesian DAG models. *The Annals of Statistics* 47 319–348. URL <https://doi.org/10.1214/18-AOS1689>. 4, 7
- CASTELLETTI, F. & CONSONNI, G. (2020a). Bayesian inference of causal effects from observational data in Gaussian graphical models. *Biometrics, In press* . 2, 23
- CASTELLETTI, F. & CONSONNI, G. (2020b). Supplementary material to “Bayesian causal inference in probit graphical models” . 3, 6, 9, 10

- DOBRA, A., HANS, C., JONES, B., NEVINS, J. R., YAO, G. & WEST, M. (2004). Sparse graphical models for exploring gene expression data. *Journal of Multivariate Analysis* 90 196 – 212. URL <http://www.sciencedirect.com/science/article/pii/S0047259X04000259>. 22
- FRIEDMAN, N. (2004). Inferring cellular networks using probabilistic graphical models. *Science* 303 799–805. URL <https://science.sciencemag.org/content/303/5659/799>. 2
- FRIEDMAN, N. & KOLLER, D. (2003). Being Bayesian about network structure. A Bayesian approach to structure discovery in Bayesian networks. *Machine Learning* 50 95–125. URL <https://doi.org/10.1023/A:1020249912095>. 2
- GARCÍA-DONATO, G. & MARTÍNEZ-BENEITO, M. A. (2013). On sampling strategies in bayesian variable selection problems with large model spaces. *Journal of the American Statistical Association* 108 340–352. URL <https://doi.org/10.1080/01621459.2012.742443>. 12
- GEIGER, D. & HECKERMAN, D. (2002). Parameter priors for directed acyclic graphical models and the characterization of several probability distributions. *The Annals of Statistics* 30 1412–1440. URL <https://doi.org/10.1214/aos/1035844981>. 8, 22
- GODSILL, S. J. (2012). On the relationship between markov chain monte carlo methods for model uncertainty. *Journal of Computational and Graphical Statistics* 10 230–248. URL <https://doi.org/10.1198/10618600152627924>. 2, 10
- GUO, J., LEVINA, E., MICHAELIDIS, G. & ZHU, J. (2015). Graphical models for ordinal data. *Journal of Computational and Graphical Statistics* 24 183–204. URL <https://doi.org/10.1080/10618600.2014.889023>. 5
- LAURITZEN, S. L. (1996). *Graphical Models*. Oxford University Press. 2, 3
- MAATHUIS, M. & NANDY, P. (2016). A review of some recent advances in causal inference. In P. Bühlmann, P. Drineas, M. Kane & M. van der Laan, eds., *Handbook of Big Data*. Chapman and Hall/CRC, 387–408. 2
- MAATHUIS, M. H., KALISCH, M. & BHLMANN, P. (2009). Estimating high-dimensional intervention effects from observational data. *The Annals of Statistics* 37 3133–3164. URL <https://doi.org/10.1214/09-AOS685>. 2, 7, 23
- MARKOWETZ, F. & SPANG, R. (2007). Inferring cellular networks - a review. *BMC Bioinformatics* 8. URL <https://doi.org/10.1186/1471-2105-8-S6-S5>. 22
- NANDY, P., MAATHUIS, M. H. & RICHARDSON, T. S. (2017). Estimating the effect of joint interventions from observational data in sparse high-dimensional settings. *Ann. Statist.* 45 647–674. URL <https://doi.org/10.1214/16-AOS1462>. 23

- OBRIEN, C. A., POLLETT, A., GALLINGER, S. & DICK, J. E. (2006). A human colon cancer cell capable of initiating tumour growth in immunodeficient mice. *Nature* 445 106–110. URL <https://doi.org/10.1038/nature05372>. 18
- PEARL, J. (1995). Causal diagrams for empirical research. *Biometrika* 82 669–688. URL <http://www.jstor.org/stable/2337329>. 2
- PEARL, J. (2000). *Causality: Models, Reasoning, and Inference*. Cambridge University Press, Cambridge. 2, 6
- PEARL, J. (2009). Causal inference in statistics: An overview. *Statistics Surveys* 3 96–146. URL <https://doi.org/10.1214/09-SS057>. 1, 2
- PETERS, J. & BÜHLMANN, P. (2014). Identifiability of Gaussian structural equation models with equal error variances. *Biometrika* 101 219–228. URL <http://www.jstor.org/stable/43305605>. 12
- PETERSON, C., STINGO, F. C. & VANNUCCI, M. (2015). Bayesian inference of multiple Gaussian graphical models. *Journal of the American Statistical Association* 110 159–174. PMID: 26078481, URL <https://doi.org/10.1080/01621459.2014.896806>. 23
- SPIRITES, P., GLYMOUR, C. & SCHEINES, R. (2000). *Causation, Prediction and Search (2nd edition)*. Cambridge, MA: The MIT Press. 4, 23
- VERMA, T. & PEARL, J. (1990). Equivalence and synthesis of causal models. In *Proceedings of the Sixth Annual Conference on Uncertainty in Artificial Intelligence*, UAI 90. New York, NY, USA: Elsevier Science Inc., 255–270. 23
- WANG, H. & LI, S. Z. (2012). Efficient gaussian graphical model determination under g-wishart prior distributions. *Electronic Journal of Statistics* 6 168–198. URL <https://doi.org/10.1214/12-EJS669>. 10
- WAUGH, D. J. & WILSON, C. (2008). The interleukin-8 pathway in cancer. *Clinical Cancer Research* 14 6735–6741. URL <https://doi.org/10.1158/1078-0432.CCR-07-4843>. 20
- XIE, Y., LIU, Y. & VALDAR, W. (2017). Joint estimation of multiple dependent Gaussian graphical models with applications to mouse genomics. *Biometrika* 103 493–511. URL <https://doi.org/10.1093/biomet/asw035>. 22
- YIN, Z.-Q., LIU, J.-J., XU, Y.-C., YU, J., DING, G.-H., YANG, F., TANG, L., LIU, B.-H., MA, Y., XIA, Y.-W., LIN, X.-L. & WANG, H.-X. (2014). A 41-gene signature derived from breast cancer stem cells as a predictor of survival. *Journal of Experimental & Clinical Cancer Research* 33. URL <https://doi.org/10.1186/1756-9966-33-49>. 17

Supplement to Bayesian causal inference in probit graphical models

Federico Castelletti, Guido Consonni

1 Proof of Proposition 3.1

In this section we give a proof of Proposition 3.1. To this end we first introduce the following two lemmata.

Lemma 1.1. *Let $\mathbf{x}, \mathbf{b} \in \mathbb{R}^d$ be two vectors, $\mathbf{M} \in \mathbb{R}^{d \times d}$ a symmetric and invertible matrix. Then*

$$\mathbf{x}^\top \mathbf{M} \mathbf{x} - 2\mathbf{b}^\top \mathbf{x} = (\mathbf{x} - \mathbf{M}^{-1}\mathbf{b})^\top \mathbf{M} (\mathbf{x} - \mathbf{M}^{-1}\mathbf{b}) - \mathbf{b}^\top \mathbf{M}^{-1}\mathbf{b}.$$

Proof. Simply expand the right-hand side of the equation. □

Lemma 1.2. *Let $V \mid (\mathbf{U} = \mathbf{u}) \sim \mathcal{N}(\mu + \boldsymbol{\gamma}^\top \mathbf{u}, \delta^2)$, $\mathbf{U} \sim \mathcal{N}_d(\mathbf{0}, \boldsymbol{\Sigma})$. Then*

$$V \sim \mathcal{N}\left(\mu, \frac{\delta^2}{1 - (\boldsymbol{\gamma}^\top \mathbf{T}^{-1} \boldsymbol{\gamma}) / \delta^2}\right),$$

where $\mathbf{T} = \boldsymbol{\Sigma}^{-1} + \boldsymbol{\gamma} \boldsymbol{\gamma}^\top / \delta^2$.

Proof. We can write by definition

$$\begin{aligned} f(v) &= \int f(v \mid \mathbf{u}) f(\mathbf{u}) d\mathbf{u} \\ &= \int_{\mathbb{R}^d} \frac{1}{\sqrt{2\pi}\delta} \exp\left\{-\frac{1}{2\delta^2}(v - \mu - \boldsymbol{\gamma}^\top \mathbf{u})^2\right\} \\ &\quad \cdot \frac{1}{(2\pi)^{d/2} |\boldsymbol{\Sigma}|^{1/2}} \exp\left\{-\frac{1}{2} \mathbf{u}^\top \boldsymbol{\Sigma}^{-1} \mathbf{u}\right\} d\mathbf{u}. \end{aligned}$$

Next, observe that

$$\begin{aligned} -\frac{1}{2\delta^2}(v - \mu - \boldsymbol{\gamma}^\top \mathbf{u})^2 &= -\frac{1}{2\delta^2} \left[(v - \mu)^2 + (\boldsymbol{\gamma}^\top \mathbf{u})^2 - 2(v - \mu) \boldsymbol{\gamma}^\top \mathbf{u} \right] \\ &= -\frac{1}{2\delta^2} \left[(v - \mu)^2 + \mathbf{u}^\top \boldsymbol{\gamma} \boldsymbol{\gamma}^\top \mathbf{u} - 2(v - \mu) \boldsymbol{\gamma}^\top \mathbf{u} \right] \\ &= -\frac{1}{2\delta^2} \left[(v - \mu)^2 + \mathbf{u}^\top \boldsymbol{\Gamma} \mathbf{u} - 2(v - \mu) \boldsymbol{\gamma}^\top \mathbf{u} \right], \end{aligned}$$

being $\boldsymbol{\Gamma} = \boldsymbol{\gamma} \boldsymbol{\gamma}^\top$. Therefore we can write

$$\begin{aligned} f(v) &= \frac{1}{\sqrt{2\pi}\delta} \exp\left\{-\frac{1}{2} \left(\frac{v - \mu}{\delta}\right)^2\right\} \\ &\quad \cdot \frac{1}{|\boldsymbol{\Sigma}|^{1/2}} \int_{\mathbb{R}^d} \frac{1}{(2\pi)^{d/2}} \exp\left\{-\frac{1}{2} \left[\mathbf{u}^\top \left(\boldsymbol{\Sigma}^{-1} + \frac{\boldsymbol{\Gamma}}{\delta^2} \right) \mathbf{u} - 2\frac{(v - \mu)}{\delta^2} \boldsymbol{\gamma}^\top \mathbf{u} \right] \right\} d\mathbf{u}. \end{aligned}$$

Let now $\mathbf{T} = \boldsymbol{\Sigma}^{-1} + \boldsymbol{\Gamma}/\delta^2$. By Lemma 1.1 we obtain

$$\begin{aligned} \mathbf{u}^\top \mathbf{T} \mathbf{u} - 2 \left[\frac{(v - \mu)}{\delta^2} \boldsymbol{\gamma}^\top \right] \mathbf{u} &= \left[\mathbf{u} - \mathbf{T}^{-1} \frac{(v - \mu)}{\delta^2} \boldsymbol{\gamma} \right]^\top \mathbf{T} \left[\mathbf{u} - \mathbf{T}^{-1} \frac{(v - \mu)}{\delta^2} \boldsymbol{\gamma} \right] \\ &\quad - \left[\frac{(v - \mu)}{\delta^2} \boldsymbol{\gamma}^\top \right] \mathbf{T}^{-1} \left[\frac{(v - \mu)}{\delta^2} \boldsymbol{\gamma} \right]. \end{aligned}$$

Therefore,

$$\begin{aligned} f(v) &= \frac{1}{\sqrt{2\pi}\delta} \exp \left\{ -\frac{1}{2} \left(\frac{v - \mu}{\delta} \right)^2 \right\} \\ &\quad \cdot \frac{1}{|\boldsymbol{\Sigma}|^{1/2}} \int_{\mathbb{R}^d} \frac{1}{(2\pi)^{d/2}} \exp \left\{ -\frac{1}{2} \left[\left(\mathbf{u} - \mathbf{T}^{-1} \frac{(v - \mu)}{\delta^2} \boldsymbol{\gamma} \right)^\top \mathbf{T} \left(\mathbf{u} - \mathbf{T}^{-1} \frac{(v - \mu)}{\delta^2} \boldsymbol{\gamma} \right) \right] \right\} \\ &\quad \cdot \exp \left\{ \frac{1}{2} \left[\frac{(v - \mu)}{\delta^2} \boldsymbol{\gamma}^\top \right] \mathbf{T}^{-1} \left[\frac{(v - \mu)}{\delta^2} \boldsymbol{\gamma} \right] \right\} d\mathbf{u}. \end{aligned}$$

Moreover we can write

$$\begin{aligned} f(v) &= \frac{1}{\sqrt{2\pi}\delta} \exp \left\{ -\frac{1}{2} \left(\frac{v - \mu}{\delta} \right)^2 \right\} \cdot \frac{1}{|\boldsymbol{\Sigma}|^{1/2}} \exp \left\{ \frac{1}{2} \left[\frac{(v - \mu)}{\delta^2} \boldsymbol{\gamma}^\top \right] \mathbf{T}^{-1} \left[\frac{(v - \mu)}{\delta^2} \boldsymbol{\gamma} \right] \right\} \\ &\quad \cdot \frac{1}{|\mathbf{T}|^{1/2}} \int_{\mathbb{R}^d} \frac{|\mathbf{T}|^{1/2}}{(2\pi)^{d/2}} \exp \left\{ -\frac{1}{2} \left(\mathbf{u} - \frac{(v - \mu)}{\delta^2} \mathbf{T}^{-1} \boldsymbol{\gamma} \right)^\top \mathbf{T} \left(\mathbf{u} - \frac{(v - \mu)}{\delta^2} \mathbf{T}^{-1} \boldsymbol{\gamma} \right) \right\} d\mathbf{u}. \end{aligned}$$

Hence,

$$f(v) = \frac{1}{\sqrt{2\pi}\delta} \frac{1}{|\boldsymbol{\Sigma}|^{1/2} |\mathbf{T}|^{1/2}} \exp \left\{ -\frac{1}{2\delta^2} \left[1 - \frac{1}{\delta^2} \boldsymbol{\gamma}^\top \mathbf{T}^{-1} \boldsymbol{\gamma} \right] (v - \mu)^2 \right\},$$

and so

$$V \sim \mathcal{N} \left(\mu, \frac{\delta^2}{1 - (\boldsymbol{\gamma}^\top \mathbf{T}^{-1} \boldsymbol{\gamma})/\delta^2} \right).$$

□

Proof of Proposition 3.1. Let $(X_1, X_2, \dots, X_q) | \boldsymbol{\Sigma} \sim (\mathbf{0}, \boldsymbol{\Sigma})$ and consider the do operator $\text{do}(X_s = \tilde{x})$ where $s \in \{2, \dots, q\}$ is the intervened node. The post-intervention distribution of X_1 is given by (Section 3)

$$f(x_1 | \text{do}(X_s = \tilde{x}), \boldsymbol{\Sigma}) = \int \mathcal{N}(x_1 | \gamma_s \tilde{x} + \boldsymbol{\gamma}^\top \mathbf{x}_{\text{pa}(s)}, \boldsymbol{\Sigma}) \cdot \mathcal{N}(\mathbf{x}_{\text{pa}(s)} | \mathbf{0}, \boldsymbol{\Sigma}_{\text{pa}(s), \text{pa}(s)}) d\mathbf{x}_{\text{pa}(s)},$$

where

$$\begin{aligned} X_1 | \mathbf{X}_{\text{pa}(s)} = \mathbf{x}_{\text{pa}(s)} &\sim \mathcal{N}(\gamma_s \tilde{x} + \boldsymbol{\gamma}^\top \mathbf{x}_{\text{pa}(s)}, \delta^2), \\ \mathbf{X}_{\text{pa}(s)} &\sim \mathcal{N}(\mathbf{0}, \boldsymbol{\Sigma}_{\text{pa}(s), \text{pa}(s)}). \end{aligned}$$

Applying Lemma 1.2 with $V = X_1$ and $\mathbf{U} = \mathbf{X}_{\text{pa}(s)}$ we obtain

$$X_1 | \text{do}(X_s = \tilde{x}), \boldsymbol{\Sigma} = \mathcal{N} \left(\gamma_s \tilde{x}, \frac{\delta^2}{1 - (\boldsymbol{\gamma}^\top \mathbf{T}^{-1} \boldsymbol{\gamma})/\delta^2} \right),$$

where

$$\begin{aligned}\delta^2 &= \Sigma_{1|\text{fa}(s)}, \\ (\gamma_s, \gamma^\top)^\top &= \Sigma_{1,\text{fa}(s)} (\Sigma_{\text{fa}(s),\text{fa}(s)})^{-1}, \\ \mathbf{T} &= (\Sigma_{\text{pa}(s),\text{pa}(s)})^{-1} + \frac{1}{\delta^2} \gamma \gamma^\top.\end{aligned}$$

□

2 PAS algorithm

We first summarize the main features of a *Partial Analytic Structure* (PAS) algorithm (Godsill, 2012; Wang & Li, 2012). Let X_1, \dots, X_q be a collection of variables, \mathbf{X} a (n, q) data matrix collecting n i.i.d. multivariate observations from X_1, \dots, X_q . Consider K distinct models, $\mathcal{M}_1, \dots, \mathcal{M}_K$, each one indexed by a parameter $\boldsymbol{\theta}_k \in \Theta_k$ and assume model uncertainty, so that the true data generating model is one of the K models. Under each model \mathcal{M}_k the likelihood function is $f(\mathbf{X} | \boldsymbol{\theta}_k, \mathcal{M}_k)$.

Consider now two models $\mathcal{M}_h, \mathcal{M}_k$, $h, k \in \{1, \dots, K\}$, $h \neq k$, with parameters $\boldsymbol{\theta}_h, \boldsymbol{\theta}_k$ and let $(\boldsymbol{\theta}_h)_u, (\boldsymbol{\theta}_k)_u$ be two sub-vector of $\boldsymbol{\theta}_h, \boldsymbol{\theta}_k$ respectively. A general PAS algorithm relies on the following two assumptions:

1. the full conditional distribution of $(\boldsymbol{\theta}_k)_u$, $p((\boldsymbol{\theta}_k)_u | (\boldsymbol{\theta}_k)_{-u}, \mathcal{M}_k, \mathbf{X})$ is available in closed form;
2. in \mathcal{M}_h there exists an “equivalent” set of parameters $(\boldsymbol{\theta}_h)_u$ with same dimension of $(\boldsymbol{\theta}_k)_u$;

see also Wang & Li (2012, Section 5.2). A PAS reversible jump algorithm adopts a proposal distribution which sets $(\boldsymbol{\theta}_h)_{-u} = (\boldsymbol{\theta}_k)_{-u}$, draws \mathcal{M}_k from $q(\mathcal{M}_k | \mathcal{M}_h)$ and $(\boldsymbol{\theta}_k)_u$ from $p((\boldsymbol{\theta}_k)_u | (\boldsymbol{\theta}_k)_{-u}, \mathcal{M}_k, \mathbf{X})$. Specifically, the update of model \mathcal{M}_k and model parameter $\boldsymbol{\theta}_k$ is performed in two steps. The first step concerns the model update and can be summarized as follows:

1. propose $\mathcal{M}_k \sim q(\mathcal{M}_k | \mathcal{M}_h)$ and set $(\boldsymbol{\theta}_h)_{-u} = (\boldsymbol{\theta}_k)_{-u}$;
2. accept \mathcal{M}_k with probability $\alpha = \min\{1, r_k\}$,

$$r_k = \frac{p(\mathcal{M}_k | (\boldsymbol{\theta}_k)_{-u}, \mathbf{X}) q(\mathcal{M}_h | \mathcal{M}_k)}{p(\mathcal{M}_h | (\boldsymbol{\theta}_h)_{-u}, \mathbf{X}) q(\mathcal{M}_k | \mathcal{M}_h)}, \quad (1)$$

where

$$p(\mathcal{M}_k | (\boldsymbol{\theta}_k)_{-u}, \mathbf{X}) = \int p(\mathcal{M}_k, (\boldsymbol{\theta}_k)_u | (\boldsymbol{\theta}_k)_{-u}, \mathbf{X}) d(\boldsymbol{\theta}_k)_u \quad (2)$$

3. if \mathcal{M}_k is accepted, generate $(\boldsymbol{\theta}_k)_u \sim p((\boldsymbol{\theta}_k)_u | (\boldsymbol{\theta}_k)_{-u}, \mathcal{M}_k, \mathbf{X})$,
otherwise $(\boldsymbol{\theta}_h)_u \sim p((\boldsymbol{\theta}_h)_u | (\boldsymbol{\theta}_h)_{-u}, \mathcal{M}_h, \mathbf{X})$.

In the second step we then update parameter $\boldsymbol{\theta}_k$ (if \mathcal{M}_k is accepted in the model update step) or $\boldsymbol{\theta}_h$ (otherwise) from its full conditional distribution using standard MCMC steps. Notice that in the case of Gaussian undirected graphical models with G-Wishart priors this requires specific MCMC techniques to avoid the computation of prior normalizing constants which are not available in closed form; see (Wang & Li, 2012, Section 2.4).

We now apply the PAS algorithm to our DAG setting. We start defining a suitable proposal distribution, $q(\mathcal{D}' | \mathcal{D})$ on the DAG space. To this end we consider three types of operators that locally modify a given DAG \mathcal{D} : insert a directed edge (InsertD $a \rightarrow b$ for short), delete a directed edge (DeleteD $a \rightarrow b$) and reverse a directed edge (ReverseD $a \rightarrow b$). For each $\mathcal{D} \in \mathcal{S}_q$, being \mathcal{S}_q the set of all DAGs on q nodes, we then construct the set of *valid* operators $\mathcal{O}_{\mathcal{D}}$, that is operators whose resulting graph is a DAG. Therefore, given the current \mathcal{D} we propose \mathcal{D}' by uniformly sampling a DAG in $\mathcal{O}_{\mathcal{D}}$. Because there is a one-to-one correspondence between each operator and resulting DAG \mathcal{D}' , the probability of transition is given by $q(\mathcal{D}' | \mathcal{D}) = 1/|\mathcal{O}_{\mathcal{D}}|$. Such a proposal can be easily adapted to account for sparsity constraints on the DAG space, for instance by fixing a maximum number of edges and limiting the model space to those DAGs having at most a given number of edges, typically a small multiple of the number of nodes.

Because of the structure of our proposal, at each step of our MCMC algorithm we will need to compare two DAGs \mathcal{D} , \mathcal{D}' which differ by one edge only. Notice that the ReverseD $a \rightarrow b$ operator can be also brought back to the same case since is equivalent to the consecutive application of the operators DeleteD $a \rightarrow b$ and InsertD $b \rightarrow a$. Therefore, consider two DAGs $\mathcal{D} = (V, E)$, $\mathcal{D}' = (V, E')$ such that $E' = E \setminus \{(h, j)\}$. Notice that if a parent ordering is valid for \mathcal{D} , it is also valid for \mathcal{D}' , and we adopt this convention to simplify the analysis. At this stage, for better clarity of notation, we index each parameter with its own DAG-model and write accordingly $(\mathbf{D}^{\mathcal{D}}, \mathbf{L}^{\mathcal{D}})$ and $(\mathbf{D}^{\mathcal{D}'}, \mathbf{L}^{\mathcal{D}'})$ and $\boldsymbol{\Omega}^{\mathcal{D}}$ and $\boldsymbol{\Omega}^{\mathcal{D}'}$ when interest centers on the covariance matrix. Notice that the Cholesky parameters under the two DAGs differ only with regard to their j -th component $((\sigma_j^{\mathcal{D}})^2, \mathbf{L}_{\prec j}^{\mathcal{D}})$, and $((\sigma_j^{\mathcal{D}'})^2, \mathbf{L}_{\prec j}^{\mathcal{D}'})$ respectively. Moreover the remaining parameters $\{(\sigma_r^{\mathcal{D}})^2, \mathbf{L}_{\prec r}^{\mathcal{D}}; r \neq j\}$ and $\{(\sigma_r^{\mathcal{D}'})^2, \mathbf{L}_{\prec r}^{\mathcal{D}'}; r \neq j\}$ are componentwise *equivalent* between the two graphs because they refer to structurally equivalent conditional models; see (6). This is crucial for the correct application of the PAS algorithm.

The acceptance probability for \mathcal{D}' under a PAS algorithm is given by $\alpha_{\mathcal{D}'} = \min\{1; r_{\mathcal{D}'}\}$ where

$$\begin{aligned} r_{\mathcal{D}'} &= \frac{p(\mathcal{D}' | \mathbf{D}^{\mathcal{D}'} \setminus (\sigma_j^{\mathcal{D}'})^2, \mathbf{L}^{\mathcal{D}'} \setminus \mathbf{L}_{\prec j}^{\mathcal{D}'}, \mathbf{X})}{p(\mathcal{D} | \mathbf{D}^{\mathcal{D}} \setminus (\sigma_j^{\mathcal{D}})^2, \mathbf{L}^{\mathcal{D}} \setminus \mathbf{L}_{\prec j}^{\mathcal{D}}, \mathbf{X})} \cdot \frac{q(\mathcal{D} | \mathcal{D}')}{q(\mathcal{D}' | \mathcal{D})} \\ &= \frac{p(\mathbf{X}, \mathbf{D}^{\mathcal{D}'} \setminus (\sigma_j^{\mathcal{D}'})^2, \mathbf{L}^{\mathcal{D}'} \setminus \mathbf{L}_{\prec j}^{\mathcal{D}'} | \mathcal{D}')}{p(\mathbf{X}, \mathbf{D}^{\mathcal{D}} \setminus (\sigma_j^{\mathcal{D}})^2, \mathbf{L}^{\mathcal{D}} \setminus \mathbf{L}_{\prec j}^{\mathcal{D}} | \mathcal{D})} \cdot \frac{p(\mathcal{D}')}{p(\mathcal{D})} \cdot \frac{q(\mathcal{D} | \mathcal{D}')}{q(\mathcal{D}' | \mathcal{D})}. \end{aligned} \quad (3)$$

Therefore we require to evaluate for DAG \mathcal{D}

$$p(\mathbf{X}, \mathbf{D} \setminus \sigma_j^2, \mathbf{L} \setminus \mathbf{L}_{\prec j} | \mathcal{D}) = \int_0^\infty \int_{\mathbb{R}^{|\text{pa}(j)|}} p(\mathbf{X} | \mathbf{D}, \mathbf{L}, \mathcal{D}) p(\mathbf{D}, \mathbf{L} | \mathcal{D}) d\mathbf{L}_{\prec j} d\sigma_j^2$$

(and similarly for \mathcal{D}') where we removed for simplicity the super-script \mathcal{D} from the Cholesky parameters, now emphasizing the dependence on \mathcal{D} though the conditioning sets. Moreover, because of the likelihood and prior factorization in (8) and (16) we can write

$$\begin{aligned} p(\mathbf{X}, \mathbf{D} \setminus \sigma_j^2, \mathbf{L} \setminus \mathbf{L}_{\prec j} | \mathcal{D}) &= \prod_{r \neq j} f(\mathbf{X}_r | \mathbf{X}_{\text{pa}(r)}, \sigma_r^2, \mathbf{L}_{\prec r}, \mathcal{D}) p(\mathbf{L}_{\prec r} | \sigma_r^2, \mathcal{D}) p(\sigma_r^2 | \mathcal{D}) \\ &\cdot \int_0^\infty \int_{\mathbb{R}^{|\text{pa}(j)|}} f(\mathbf{X}_j | \mathbf{X}_{\text{pa}(j)}, \sigma_j^2, \mathbf{L}_{\prec j}, \mathcal{D}) \\ &\cdot p(\mathbf{L}_{\prec j} | \sigma_j^2, \mathcal{D}) p(\sigma_j^2 | \mathcal{D}) d\mathbf{L}_{\prec j} d\sigma_j^2. \end{aligned} \quad (4)$$

In particular, because of conjugacy of the Normal density with the Normal-Inverse-Gamma prior, the integral in (4) can be obtained in closed form as

$$m(\mathbf{X}_j | \mathbf{X}_{\text{pa}_{\mathcal{D}}(j)}, \mathcal{D}) = (2\pi)^{-\frac{n}{2}} \frac{|\mathbf{T}_j|^{1/2}}{|\bar{\mathbf{T}}_j|^{1/2}} \cdot \frac{\Gamma\left(a_j^* + \frac{n}{2}\right)}{\Gamma\left(a_j^*\right)} \left[\frac{1}{2}g\right]^{a_j^*} \left[\frac{1}{2}(g + \mathbf{X}_j^\top \mathbf{X}_j - \hat{\mathbf{L}}_j^\top \bar{\mathbf{T}}_j \hat{\mathbf{L}}_j)\right]^{-(a_j^* + n/2)} \quad (5)$$

where

$$\begin{aligned} \mathbf{T}_j &= g\mathbf{I}_{|\text{pa}_{\mathcal{D}}(j)|} \\ \bar{\mathbf{T}}_j &= g\mathbf{I}_{|\text{pa}_{\mathcal{D}}(j)|} + \mathbf{X}_{\text{pa}_{\mathcal{D}}(j)}^\top \mathbf{X}_{\text{pa}_{\mathcal{D}}(j)} \\ \hat{\mathbf{L}}_j &= (g\mathbf{I}_{|\text{pa}_{\mathcal{D}}(j)|} + \mathbf{X}_{\text{pa}_{\mathcal{D}}(j)}^\top \mathbf{X}_{\text{pa}_{\mathcal{D}}(j)})^{-1} \mathbf{X}_{\text{pa}_{\mathcal{D}}(j)}^\top \mathbf{X}_j, \end{aligned}$$

and $a_j^* = \frac{a_j}{2} - \frac{|\text{pa}_{\mathcal{D}}(j)|}{2} - 1$. For $j = 1$, because we fixed $\sigma_1^2 = 1$ we instead obtain

$$m(\mathbf{X}_1 | \mathbf{X}_{\text{pa}_{\mathcal{D}}(1)}, \mathcal{D}) = (2\pi)^{-\frac{n}{2}} \frac{|\mathbf{T}_1|^{1/2}}{|\bar{\mathbf{T}}_1|^{1/2}} \cdot \exp\left\{-\frac{1}{2}(\mathbf{X}_1^\top \mathbf{X}_1 + \hat{\mathbf{L}}_1^\top \bar{\mathbf{T}}_1 \hat{\mathbf{L}}_1)\right\}. \quad (6)$$

Therefore, the PAS ratio in (3) reduces to

$$r_{\mathcal{D}'} = \frac{m(\mathbf{X}_j | \mathbf{X}_{\text{pa}_{\mathcal{D}'}(j)}, \mathcal{D}')}{m(\mathbf{X}_j | \mathbf{X}_{\text{pa}_{\mathcal{D}}(j)}, \mathcal{D})} \cdot \frac{p(\mathcal{D}')}{p(\mathcal{D})} \cdot \frac{q(\mathcal{D} | \mathcal{D}')}{q(\mathcal{D}' | \mathcal{D})}. \quad (7)$$

3 Proof of Proposition 4.1

In this section we prove that the posterior distribution $p(\mathbf{D}, \mathbf{L}, \mathcal{D}, \theta_0, \mathbf{X}_1 | \mathbf{y}, \mathbf{X}_{-1})$ is proper. To this end we factorize it as

$$\begin{aligned} p(\mathbf{D}, \mathbf{L}, \mathcal{D}, \theta_0, \mathbf{X}_1 | \mathbf{y}, \mathbf{X}_{-1}) &\propto p(\theta_0 | \mathbf{y}, \mathbf{X}_{-1}) p(\mathbf{X}_1 | \theta_0, \mathbf{y}, \mathbf{X}_{-1}) \\ &\cdot p(\mathbf{D}, \mathbf{L} | \theta_0, \mathbf{X}_1, \mathbf{y}, \mathbf{X}_{-1}) p(\mathcal{D} | \mathbf{D}, \mathbf{L}, \theta_0, \mathbf{X}_1, \mathbf{y}, \mathbf{X}_{-1}). \end{aligned}$$

Also, because \mathbf{y} is deterministically set once \mathbf{X}_1 and θ_0 are given, the latter simplifies to

$$\begin{aligned} p(\mathbf{D}, \mathbf{L}, \mathcal{D}, \theta_0, \mathbf{X}_1 | \mathbf{y}, \mathbf{X}_{-1}) &\propto p(\theta_0 | \mathbf{y}, \mathbf{X}_{-1}) p(\mathbf{X}_1 | \theta_0, \mathbf{y}, \mathbf{X}_{-1}) \\ &\cdot p(\mathbf{D}, \mathbf{L} | \theta_0, \mathbf{X}) p(\mathcal{D} | \mathbf{D}, \mathbf{L}, \theta_0, \mathbf{X}), \end{aligned}$$

where \mathbf{X} is the (n, q) augmented data matrix, column binding of \mathbf{X}_1 and \mathbf{X}_{-1} . To prove the propriety of the joint posterior we will show that each of the above terms corresponds to a proper distribution.

3.1 Propriety of $p(\theta_0 | \mathbf{y}, \mathbf{X}_{-1})$

First notice that $p(\theta_0 | \mathbf{y}, \mathbf{X}_{-1}) \propto p(\mathbf{y}, \mathbf{X}_{-1} | \theta_0)$ since $p(\theta_0) \propto 1$. Remember the *augmented* likelihood in Equation (9) of our manuscript

$$f(\mathbf{y}, \mathbf{X} | \mathbf{D}, \mathbf{L}, \theta_0, \mathcal{D}) = \prod_{j=1}^q d\mathcal{N}_n(\mathbf{X}_j | -\mathbf{X}_{\text{pa}(j)} \mathbf{L}_{\prec j}, \sigma_j^2 \mathbf{I}_n) \cdot \left\{ \prod_{i=1}^n \mathbb{1}(\theta_{y_i-1} < x_{i,1} \leq \theta_{y_i}) \right\},$$

now emphasizing the dependence on DAG \mathcal{D} , where we set the (j, j) -element of \mathbf{D} equal to σ_j^2 . We first integrate out \mathbf{X}_1 to obtain the likelihood

$$\begin{aligned} f(\mathbf{y}, \mathbf{X}_{-1} | \mathbf{D}, \mathbf{L}, \theta_0, \mathcal{D}) &= \prod_{j=2}^q d\mathcal{N}_n(\mathbf{X}_j | -\mathbf{X}_{\text{pa}(j)} \mathbf{L}_{\prec j}, \sigma_j^2 \mathbf{I}_n) \\ &\cdot \int_{\mathbb{R}^n} d\mathcal{N}_n(\mathbf{X}_1 | -\mathbf{X}_{\text{pa}(1)} \mathbf{L}_{\prec 1}, \sigma_1^2 \mathbf{I}_n) \prod_{i=1}^n \mathbb{1}(\theta_{y_i-1} < x_{i,1} \leq \theta_{y_i}) d\mathbf{X}_1 \\ &= f(\mathbf{X}_{-1} | \mathbf{D}, \mathbf{L}) \cdot \int_{O^n(\mathbf{y}, \theta_0)} d\mathcal{N}_n(\mathbf{X}_1 | -\mathbf{X}_{\text{pa}(1)} \mathbf{L}_{\prec 1}, \sigma_1^2 \mathbf{I}_n) d\mathbf{X}_1, \end{aligned}$$

where $\mathbf{X}_{-1} = (\mathbf{X}_2, \dots, \mathbf{X}_q)$, $O^n(\mathbf{y}, \theta_0)$ is the n -dimensional orthant $\bigtimes_{i=1}^n (\theta_{y_i-1}, \theta_{y_i}]$ and $\theta_{-1} = -\infty, \theta_1 = +\infty$. To obtain the marginal posterior of θ_0 we first compute the *integrated likelihood* for θ_0 by integrating the likelihood w.r.t. (\mathbf{D}, \mathbf{L}) . Because of prior parameter independence across $(\sigma_j^2, \mathbf{L}_{\prec j})$'s, we obtain

$$\begin{aligned} f(\mathbf{y}, \mathbf{X}_{-1} | \theta_0) &= \int f(\mathbf{y}, \mathbf{X}_{-1} | \mathbf{D}, \mathbf{L}, \theta_0) p(\mathbf{D}, \mathbf{L}) d\mathbf{D} d\mathbf{L} \\ &= \prod_{j=2}^q \left\{ \int d\mathcal{N}_n(\mathbf{X}_j | -\mathbf{X}_{\text{pa}(j)} \mathbf{L}_{\prec j}, \sigma_j^2 \mathbf{I}_n) p(\sigma_j^2, \mathbf{L}_{\prec j}) d\sigma_j^2 d\mathbf{L}_{\prec j} \right\} \\ &\cdot \int_{\mathbb{R}^{|\text{pa}(1)|}} \int_{O^n(\mathbf{y}, \theta_0)} d\mathcal{N}_n(\mathbf{X}_1 | -\mathbf{X}_{\text{pa}(1)} \mathbf{L}_{\prec 1}, \sigma_1^2 \mathbf{I}_n) p(\mathbf{L}_{\prec 1}) d\mathbf{X}_1 d\mathbf{L}_{\prec 1}, \end{aligned}$$

since $\sigma_1^2 = 1$. Notice that the first term in the integrated likelihood $f(\mathbf{y}, \mathbf{X}_{-1} | \theta_0)$ does not depend on θ_0 . We then write

$$f(\mathbf{y}, \mathbf{X}_{-1} | \theta_0) = K(\mathbf{X}_{-1}) \cdot \int_{O^n(\mathbf{y}, \theta_0)} \int_{\mathbb{R}^{|\text{pa}(1)|}} d\mathcal{N}_n(\mathbf{X}_1 | -\mathbf{X}_{\text{pa}(1)} \mathbf{L}_{\prec 1}, \sigma_1^2 \mathbf{I}_n) p(\mathbf{L}_{\prec 1}) d\mathbf{L}_{\prec 1} d\mathbf{X}_1,$$

upon interchanging the order of integration. Consider now the inner integral where $p(\mathbf{L}_{\prec 1}) = d\mathcal{N}_{|\text{pa}(1)|}(\mathbf{0}, g^{-1} \mathbf{I}_{\text{pa}(1)})$; see also Equation (15) in our manuscript. Because of conjugacy with the normal density $d\mathcal{N}_n(\mathbf{X}_1 | \cdot)$ we obtain

$$\int_{\mathbb{R}^{|\text{pa}(1)|}} d\mathcal{N}_n(\mathbf{X}_1 | -\mathbf{X}_{\text{pa}(1)} \mathbf{L}_{\prec 1}, \sigma_1^2 \mathbf{I}_n) p(\mathbf{L}_{\prec 1}) d\mathbf{L}_{\prec 1} = d\mathcal{N}_n(\mathbf{X}_1 | \mathbf{0}, \mathbf{\Sigma}_1),$$

where $|\text{pa}(1)|$ is the number of parents, $\mathbf{\Sigma}_1 = g^{-1} \mathbf{X}_{\text{pa}(1)} \mathbf{X}_{\text{pa}(1)}^\top + \mathbf{I}_n$. The integrated likelihood thus becomes

$$f(\mathbf{y}, \mathbf{X}_{-1} | \theta_0) = K(\mathbf{X}_{-1}) \cdot \int_{O^n(\mathbf{y}, \theta_0)} d\mathcal{N}_n(\mathbf{X}_1 | \mathbf{0}, \mathbf{\Sigma}_1) d\mathbf{X}_1. \quad (8)$$

Since we assumed $p(\theta_0) \propto 1$, the marginal posterior of θ_0 is proportional to (8) and also

$$\begin{aligned} p(\theta_0 | \mathbf{y}, \mathbf{X}_{-1}) &\propto \int_{O^n(\mathbf{y}, \theta_0)} d\mathcal{N}_n(\mathbf{X}_1 | \mathbf{0}, \mathbf{\Sigma}_1) d\mathbf{X}_1 \\ &:= I(\theta_0, n), \end{aligned}$$

where we emphasize the dependence on n . Therefore, to verify the propriety of $p(\theta_0 | \mathbf{y}, \mathbf{X}_{-1})$ we need to prove that $I(\theta_0, n)$ is integrable over $\theta_0 \in (-\infty, \infty)$.

Let now for simplicity $\mathbf{X}_1 = \mathbf{U} = (U_1, \dots, U_n)^\top$ and recall that

$$\begin{aligned} U_i \in (-\infty, \theta_0] &\iff U_i \leq \theta_0 \iff U_i - \theta_0 \leq 0, \\ U_i \in (\theta_0, \infty) &\iff U_i > \theta_0 \iff \theta_0 - U_i < 0. \end{aligned}$$

Hence, if we let

$$U_i^* = \begin{cases} U_i - \theta_0 & \text{if } y_i = 0, \\ \theta_0 - U_i & \text{if } y_i = 1, \end{cases}$$

we obtain that $\mathbf{U}^* \sim \mathcal{N}_n(\boldsymbol{\mu}^*, \boldsymbol{\Sigma}^*)$, where $\boldsymbol{\mu}^* = (\mu_1^*, \dots, \mu_n^*)^\top$,

$$\mu_i^* = \begin{cases} -\theta_0 & \text{if } y_i = 0, \\ \theta_0 & \text{if } y_i = 1, \end{cases} \quad \Sigma^*(h, k) = \begin{cases} \Sigma_1(h, k) & \text{if } y_h = y_k, \\ -\Sigma_1(h, k) & \text{if } y_h \neq y_k, \end{cases}$$

and $\Sigma^*(h, k)$ denotes the element at position (h, k) in Σ^* . Therefore, we can write

$$I(\theta_0, n) = \int_0^\infty \cdots \int_0^\infty d\mathcal{N}_n(\mathbf{U}^* | \boldsymbol{\mu}^*, \boldsymbol{\Sigma}^*) dU_1^* \cdots dU_n^*. \quad (9)$$

If $n = 1$, then (9) is not integrable so that the posterior of θ_0 improper. To see why, notice that

$$\begin{aligned} I(\theta_0, 1) &= \int_0^\infty d\mathcal{N}(U_1^* | \mu^*, \sigma^{2*}) dU_1^* \\ &= \begin{cases} \Phi\left(\frac{\theta_0}{\sigma^{2*}}\right) & \text{if } y_i = 0, \\ \Phi\left(-\frac{\theta_0}{\sigma^{2*}}\right) & \text{if } y_i = 1, \end{cases} \end{aligned}$$

which is not integrable over $(-\infty, \infty)$ in either case.

Consider now $n = 2$ and assume that the two observations have different values for Y , say $y_1 = 1$ and $y_2 = 0$. We then obtain

$$\begin{pmatrix} U_2^* \\ U_1^* \end{pmatrix} \sim \mathcal{N}\left[\begin{pmatrix} \theta_0 \\ -\theta_0 \end{pmatrix}, \begin{pmatrix} \sigma_1^2 & \rho\sigma_1\sigma_2 \\ \rho\sigma_1\sigma_2 & \sigma_2^2 \end{pmatrix}\right],$$

where $\rho = \text{Corr}(U_1^*, U_2^*)$ and

$$\begin{aligned} I(\theta_0, 2) &= \int_0^\infty \int_0^\infty d\mathcal{N}_2(\mathbf{U}^* | \boldsymbol{\mu}^*, \boldsymbol{\Sigma}^*) dU_1^* dU_2^* \\ &= P\{U_1^* > 0, U_2^* > 0\}. \end{aligned}$$

The posterior for θ_0 is proper if and only if $\int_{-\infty}^\infty I(\theta_0, 2) d\theta_0 < \infty$. We will show this result by providing an upper bound $I(\theta_0, 2) \leq G(\theta_0, 2)$ with $G(\theta_0, 2)$ integrable over the real line.

To this end, we first standardize U_1^* and U_2^*

$$V_1^* = \frac{U_1^* - \theta_0}{\sigma_1}$$

$$V_2^* = \frac{U_2^* + \theta_0}{\sigma_2},$$

so that

$$\begin{pmatrix} V_1^* \\ V_2^* \end{pmatrix} \sim \mathcal{N} \left[\begin{pmatrix} 0 \\ 0 \end{pmatrix}, \begin{pmatrix} 1 & \rho \\ \rho & 1 \end{pmatrix} \right]$$

and

$$P \{U_1^* > 0, U_2^* > 0\} = P \left\{ V_1^* > -\frac{\theta_0}{\sigma_1}, V_2^* > \frac{\theta_0}{\sigma_2} \right\}. \quad (10)$$

We now distinguish two cases: $\rho \geq 0$ and $\rho < 0$.

Case 1 Consider first $0 \leq \rho < 1$. Applying Equation (C.8) in [Melchers & Beck \(2017\)](#) to the right-hand-side of (10) we obtain

$$P \{U_1^* > 0, U_2^* > 0\} \leq \Phi(-b)\Phi\left(\frac{\theta_0}{\sigma_1}\right) + \Phi(-a)\Phi\left(-\frac{\theta_0}{\sigma_2}\right) := H(\theta_0, 2),$$

where

$$a = \frac{-\theta_0 \left[\frac{1}{\sigma_1} + \frac{\rho}{\sigma_2} \right]}{(1 - \rho^2)^{1/2}}, \quad b = \frac{\theta_0 \left[\frac{1}{\sigma_2} + \frac{\rho}{\sigma_1} \right]}{(1 - \rho^2)^{1/2}},$$

and $\Phi(t)$ is the c.d.f. of a standard normal distribution evaluated at t . It follows that $H(\theta_0, 2)$ is continuous, bounded and

$$\lim_{\theta_0 \rightarrow -\infty} H(\theta_0, 2) = 0, \quad \lim_{\theta_0 \rightarrow \infty} H(\theta_0, 2) = 0.$$

Now we verify integrability of $H(\theta_0, 2)$ in a right and left neighborhood of $-\infty$ and ∞ respectively.

Consider first $\theta_0 \rightarrow -\infty$ and notice that

$$\begin{aligned} H(\theta_0, 2) &\leq \Phi\left(\frac{\theta_0}{\sigma_1}\right) + \Phi(-a) \\ &= \Phi(\theta_0 A) + \Phi(\theta_0 B) \\ &= P\{Z \geq -\theta_0 A\} + P\{Z \geq -\theta_0 B\}. \end{aligned}$$

where $Z \sim \mathcal{N}(0, 1)$ and

$$A = \frac{1}{\sigma_1} > 0 \quad B = \frac{\frac{1}{\sigma_1} + \frac{\rho}{\sigma_2}}{(1 - \rho^2)^{1/2}} > 0.$$

Because $\theta_0 \rightarrow -\infty$, we have $-\theta_0 A > 0, -\theta_0 B > 0$. Applying the following inequality for the upper tail of Z

$$P\{Z > z\} \leq \frac{\exp\{-z^2/2\}}{z\sqrt{2\pi}}, \quad z > 0,$$

one gets

$$\begin{aligned}
P\{Z \geq -\theta_0 A\} + P\{Z \geq -\theta_0 B\} &\leq \frac{\exp\{-\theta_0^2 A^2/2\}}{-\theta_0 A\sqrt{2\pi}} + \frac{\exp\{-\theta_0^2 B^2/2\}}{-\theta_0 B\sqrt{2\pi}} \\
&\leq \frac{\exp\{-\theta_0^2 A^2/2\}}{A\sqrt{2\pi}} + \frac{\exp\{-\theta_0^2 B^2/2\}}{B\sqrt{2\pi}} \\
&:= G(\theta_0, 2).
\end{aligned}$$

Clearly $\int_{-\infty}^0 G(\theta_0, 2)d\theta_0 < \infty$, whence $I(\theta_0, 2)$ is integrable in a right neighborhood of $-\infty$.

Consider now $\theta_0 \rightarrow \infty$. Similarly as before notice that

$$\begin{aligned}
H(\theta_0, 2) &\leq \Phi(-b) + \Phi\left(-\frac{\theta_0}{\sigma_2}\right) \\
&= \Phi(-\theta_0 C) + \Phi(-\theta_0 D) \\
&= P\{Z \geq \theta_0 C\} + P\{Z \geq \theta_0 D\}.
\end{aligned}$$

where

$$C = \frac{\frac{1}{\sigma_2} + \frac{\rho}{\sigma_1}}{(1 - \rho^2)^{1/2}} > 0, \quad D = \frac{1}{\sigma_2} > 0$$

It follows that an upper bound for $I(\theta_0, 2)$ is now

$$G(\theta_0, 2) = \frac{\exp\{-\theta_0^2 C^2/2\}}{C\sqrt{2\pi}} + \frac{\exp\{-\theta_0^2 D^2/2\}}{D\sqrt{2\pi}}.$$

Thus for $\rho \geq 0$ the posterior for θ_0 is proper.

Case 2 Consider now the case $-1 < \rho < 0$.

We rewrite (10) using $P_{\rho < 0}\{\cdot\}$ to indicate that the probability is evaluated w.r.t. the joint distribution when the correlation coefficient is less than zero, and use $P_{\rho \geq 0}\{\cdot\}$ otherwise. Letting $v_1 = -\frac{\theta_0}{\sigma_1}, v_2 = \frac{\theta_0}{\sigma_2}$ we have

$$\begin{aligned}
P_{\rho < 0}\{U_1^* > 0, U_2^* > 0\} &= P_{\rho < 0}\{V_1^* > v_1, V_2^* > v_2\} \\
&= P_{\rho < 0}\{V_1^* \leq v_1, V_2^* \leq v_2\} + P\{V_1^* > v_1\} + P\{V_2^* > v_2\} - 1 \\
&\leq P_{\rho \geq 0}\{V_1^* \leq v_1, V_2^* \leq v_2\} + P\{V_1^* > v_1\} + P\{V_2^* > v_2\} - 1 \\
&= P_{\rho \geq 0}\{V_1^* > v_1, V_2^* > v_2\} \\
&= P_{\rho \geq 0}\{U_1^* > 0, U_2^* > 0\};
\end{aligned}$$

see Equation (C.16) in [Melchers & Beck \(2017\)](#) for the inequality in step 3.

It follows that $I(\theta_0, 2)$ for $1 < \rho < 0$ is bounded above by the corresponding function for the case $0 \leq \rho < 1$. Hence $I(\theta_0, 2)$ is integrable also for $\rho < 0$ and propriety of the posterior of θ_0 holds in this case too.

Having established that $p(\theta_0 | \mathbf{y}, \mathbf{X}_{-1})$ is proper when $n = 2$ and $y_1 = 1, y_2 = 0$, it follows that propriety will hold for any sample size $n \geq 2$ provided that there exist at least two observations with distinct values for Y . To see why, assume without loss of generality that the first two observations have distinct values; then

$$p(\theta_0 | \mathbf{y}^{(1:n)}, \mathbf{X}_{-1}^{(1:n)}) \propto p(\theta_0 | \mathbf{y}^{(1:2)}, \mathbf{X}_{-1}^{(1:2)}) \cdot f(\mathbf{y}^{(3:n)}, \mathbf{X}_{-1}^{(3:n)} | \mathbf{y}^{(1:2)}, \mathbf{X}_{-1}^{(1:2)}, \theta_0),$$

which is proper because $p(\theta_0 | \mathbf{y}^{(1:2)}, \mathbf{X}_{-1}^{(1:2)})$ is proper and the conditional integrated likelihood $f(\cdot | \cdot)$ is not degenerate.

Results presented in the next sections rely on the following proposition.

Proposition 3.1. *Let $p(\mathbf{X} | \boldsymbol{\vartheta}, \boldsymbol{\lambda})$ be a proper statistical model for the data \mathbf{X} where $\boldsymbol{\vartheta}$, $\boldsymbol{\lambda}$ are continuous parameters with joint prior $p(\boldsymbol{\vartheta}, \boldsymbol{\lambda}) = p(\boldsymbol{\lambda} | \boldsymbol{\vartheta})p(\boldsymbol{\vartheta})$. If $p(\boldsymbol{\lambda} | \boldsymbol{\vartheta})$ is proper, then*

$$p(\mathbf{X} | \boldsymbol{\vartheta}) = \int p(\mathbf{X} | \boldsymbol{\vartheta}, \boldsymbol{\lambda}) p(\boldsymbol{\lambda} | \boldsymbol{\vartheta}) d\boldsymbol{\lambda}$$

is also a proper statistical model. If viewed as a function of $\boldsymbol{\vartheta}$, $p(\mathbf{X} | \boldsymbol{\vartheta})$ is called integrated likelihood.

Proof. The proof is immediate if one can interchange the order of integration between \mathbf{X} and $\boldsymbol{\lambda}$. \square

In addition, it follows that if $p(\boldsymbol{\vartheta})$ is also proper, then the posterior of $\boldsymbol{\vartheta}$, $p(\boldsymbol{\vartheta} | \mathbf{X})$, will also be proper.

3.2 Propriety of $p(\mathbf{X}_1 | \theta_0, \mathbf{y}, \mathbf{X}_{-1})$

We can first write

$$\begin{aligned} p(\mathbf{X}_1 | \theta_0, \mathbf{y}, \mathbf{X}_{-1}) &\propto p(\mathbf{X}_{-1} | \mathbf{y}, \theta_0, \mathbf{X}_1) p(\mathbf{y} | \theta_0, \mathbf{X}_1) p(\mathbf{X}_1 | \theta_0) \\ &= p(\mathbf{X}_{-1} | \theta_0, \mathbf{X}_1) p(\mathbf{y} | \theta_0, \mathbf{X}_1) p(\mathbf{X}_1 | \theta_0) \end{aligned}$$

since $p(\mathbf{X}_{-1} | \mathbf{y}, \theta_0, \mathbf{X}_1) = p(\mathbf{X}_{-1} | \theta_0, \mathbf{X}_1)$ and $p(\theta_0) \propto 1$.

The first term can be written as

$$p(\mathbf{X}_{-1} | \theta_0, \mathbf{X}_1) = \sum_{\mathcal{D}} \left\{ \int \int p(\mathbf{X}_{-1} | \mathbf{D}, \mathbf{L}, \mathcal{D}, \theta_0, \mathbf{X}_1) p(\mathbf{D}, \mathbf{L} | \mathcal{D}, \theta_0, \mathbf{X}_1) d\mathbf{D} d\mathbf{L} \right\} p(\mathcal{D} | \theta_0, \mathbf{X}_1).$$

Now notice that

$$\begin{aligned} p(\mathbf{D}, \mathbf{L} | \mathcal{D}, \theta_0, \mathbf{X}_1) &\propto p(\mathbf{X}_1 | \mathbf{D}, \mathbf{L}, \mathcal{D}, \theta_0) p(\mathbf{D}, \mathbf{L} | \mathcal{D}, \theta_0) \\ &\propto p(\mathbf{X}_1 | \mathbf{D}, \mathbf{L}, \mathcal{D}, \theta_0) p(\mathbf{D}, \mathbf{L} | \mathcal{D}), \end{aligned}$$

and that we can write

$$\begin{aligned} p(\mathbf{X}_1 | \mathbf{D}, \mathbf{L}, \mathcal{D}, \theta_0) &= \sum_{\mathbf{y} \in \{0,1\}^n} \left\{ \int f(\mathbf{y}, \mathbf{X} | \mathbf{D}, \mathbf{L}, \theta_0) d\mathbf{X}_{-1} \right\} \\ &= \sum_{\mathbf{y} \in \{0,1\}^n} \left\{ \int f(\mathbf{X} | \mathbf{D}, \mathbf{L}, \mathcal{D}) d\mathbf{X}_{-1} \prod_{i=1}^n \mathbb{1}(\theta_{y_i-1} < x_{i,1} \leq \theta_{y_i}) \right\} \\ &= d\mathcal{N}_n(\mathbf{X}_1 | \mathbf{0}, \tau_1^2 \mathbf{I}_n) \sum_{\mathbf{y} \in \{0,1\}^n} \left\{ \prod_{i=1}^n \mathbb{1}(\theta_{y_i-1} < x_{i,1} \leq \theta_{y_i}) \right\} \\ &= d\mathcal{N}_n(\mathbf{X}_1 | \mathbf{0}, \tau_1^2 \mathbf{I}_n), \end{aligned}$$

being $\tau_1^2 = [(\mathbf{L}^\top)^{-1} \mathbf{D} \mathbf{L}^{-1}]_{11}$, because for each fixed $\mathbf{X}_1 = (x_{1,1}, \dots, x_{n,1})^\top$ only one of the 2^n product of indicators will hold true and therefore $\sum_{\mathbf{y} \in \{0,1\}^n} \{\dots\} = 1$. Hence, $p(\mathbf{X}_1 | \mathbf{D}, \mathbf{L}, \mathcal{D}, \theta_0)$ corresponds to a (proper) multivariate normal density. Also, $p(\mathbf{D}, \mathbf{L} | \mathcal{D})$ is a proper (prior) distribution by assumption. It follows that $p(\mathbf{X}_{-1} | \theta_0, \mathbf{X}_1)$ is an integrated likelihood because it is obtained with proper priors $p(\mathbf{D}, \mathbf{L} | \mathcal{D}, \theta_0, \mathbf{X}_1)$ and $p(\mathcal{D} | \theta_0, \mathbf{X}_1)$.

Moreover, $p(\mathbf{y} | \theta_0, \mathbf{X}_1)$ is also proper because

$$p(\mathbf{y} | \theta_0, \mathbf{X}_1) = \begin{cases} 1 & \text{if } y_i = \mathbb{1}(x_{i,1} > \theta_0) \text{ for each } i = 1, \dots, n, \\ 0 & \text{otherwise.} \end{cases} \quad (11)$$

Finally we have

$$\begin{aligned} p(\mathbf{X}_1 | \theta_0) &= \sum_{\mathcal{D}} \left\{ \int \int p(\mathbf{X}_1 | \mathbf{D}, \mathbf{L}, \mathcal{D}, \theta_0) p(\mathbf{D}, \mathbf{L} | \theta_0, \mathcal{D}) d\mathbf{D} d\mathbf{L} \right\} p(\mathcal{D} | \theta_0) \\ &= \sum_{\mathcal{D}} \left\{ \int d\mathcal{N}_n(\mathbf{X}_1 | \mathbf{0}, \tau_1^2 \mathbf{I}_n) p(\tau_1^2 | \mathcal{D}) d\tau_1^2 \right\} p(\mathcal{D}), \end{aligned}$$

which is also proper because the family of densities for \mathbf{X}_1 is integrated w.r.t. proper priors $p(\tau_1^2 | \mathcal{D})$ (induced by the proper prior on (\mathbf{D}, \mathbf{L})) and $p(\mathcal{D})$.

3.3 Propriety of $p(\mathbf{D}, \mathbf{L} | \theta_0, \mathbf{X})$

Consider now

$$p(\mathbf{D}, \mathbf{L} | \theta_0, \mathbf{X}) = \sum_{\mathcal{D}} p(\mathbf{D}, \mathbf{L} | \mathcal{D}, \theta_0, \mathbf{X}) p(\mathcal{D} | \theta_0, \mathbf{X}).$$

First notice that

$$\begin{aligned} p(\mathbf{D}, \mathbf{L} | \mathcal{D}, \theta_0, \mathbf{X}) &\propto p(\mathbf{X} | \mathbf{D}, \mathbf{L}, \mathcal{D}, \theta_0) p(\mathbf{D}, \mathbf{L} | \mathcal{D}, \theta_0) \\ &= p(\mathbf{X} | \mathbf{D}, \mathbf{L}, \mathcal{D}, \theta_0) p(\mathbf{D}, \mathbf{L} | \mathcal{D}), \end{aligned}$$

where

$$\begin{aligned} p(\mathbf{X} | \mathbf{D}, \mathbf{L}, \mathcal{D}, \theta_0) &= \sum_{\mathbf{y} \in \{0,1\}^n} p(\mathbf{y}, \mathbf{X} | \mathbf{D}, \mathbf{L}, \theta_0) \\ &= \sum_{\mathbf{y} \in \{0,1\}^n} \left\{ p(\mathbf{X} | \mathbf{D}, \mathbf{L}, \mathcal{D}) \prod_{i=1}^n \mathbb{1}(\theta_{y_i-1} < x_{i,1} \leq \theta_{y_i}) \right\} \\ &= p(\mathbf{X} | \mathbf{D}, \mathbf{L}, \mathcal{D}), \end{aligned}$$

arguing as in Section 3.2. Therefore we can write $p(\mathbf{D}, \mathbf{L} | \mathcal{D}, \theta_0, \mathbf{X}) = p(\mathbf{D}, \mathbf{L} | \mathcal{D}, \mathbf{X})$ which is a proper DAG Wishart distribution.

In addition, $p(\mathcal{D} | \theta_0, \mathbf{X}) \propto p(\mathbf{X} | \mathcal{D}, \theta_0) p(\mathcal{D} | \theta_0) = p(\mathbf{X} | \mathcal{D}, \theta_0) p(\mathcal{D})$ where

$$\begin{aligned} p(\mathbf{X} | \theta_0, \mathcal{D}) &= \int \int p(\mathbf{X} | \mathbf{D}, \mathbf{L}, \mathcal{D}, \theta_0) p(\mathbf{D}, \mathbf{L} | \mathcal{D}, \theta_0) d\mathbf{D} d\mathbf{L} \\ &= \int \int p(\mathbf{X} | \mathbf{D}, \mathbf{L}, \mathcal{D}) p(\mathbf{D}, \mathbf{L} | \mathcal{D}) d\mathbf{D} d\mathbf{L} \end{aligned}$$

is again an integrated (augmented) likelihood with a proper prior $p(\mathbf{D}, \mathbf{L} | \mathcal{D})$ and therefore proper. Hence, $p(\mathcal{D} | \theta_0, \mathbf{X})$ is proper according to Proposition 3.1 because $p(\mathcal{D})$ is also a proper prior.

Therefore, $p(\mathbf{D}, \mathbf{L} | \theta_0, \mathbf{X})$ is proper because it corresponds to a finite mixture of proper priors.

3.4 Propriety of $p(\mathcal{D} | \mathbf{D}, \mathbf{L}, \theta_0, \mathbf{X})$

Finally, we can write

$$\begin{aligned} p(\mathcal{D} | \mathbf{D}, \mathbf{L}, \theta_0, \mathbf{X}) &\propto p(\mathbf{X} | \mathbf{D}, \mathbf{L}, \mathcal{D}, \theta_0) p(\mathcal{D} | \theta_0) \\ &= p(\mathbf{X} | \mathbf{D}, \mathbf{L}, \mathcal{D}) p(\mathcal{D}), \end{aligned}$$

which will be proper because \mathcal{D} belongs to a finite space.

4 MCMC convergence diagnostics

In order to fix the number of MCMC iterations in our simulation study we have run few pilot simulations that we used to perform diagnostics of convergence. Specifically, for each pilot simulation we ran two independent chains of length T_1 and T_2 . We fixed $T_1 = 25000$ and $T_2 = 50000$ in the $q = 20$ setting, while $T_1 = 50000$ and $T_2 = 100000$ for $q = 40$.

We compare the BMA causal effect estimates (as defined in Equation (27) of our paper) obtained under the two independent chains. Figure 1 shows the scatter plots of the BMA estimates obtained from the two chains for four randomly chosen intervened nodes in one of the pilot simulations for $q = 20$. By inspection, one can see that the agreement between the results is highly satisfactory since points are clustered around the main diagonal of the plot. Therefore, T_1 iterations are sufficient to reach convergence. Similar results, not reported for brevity, were obtained in the $q = 40$ scenarios.

5 Simulation results and comparisons

To emphasize the crucial role played by the set $fa(s)$ in causal effect estimation, we compare our method with an alternative setup which does not adjust for confounders. Specifically, we perform inference of causal effects under a fixed *naive* DAG wherein all variables, save for the response, are disjoint and each is a parent of the response; see Figure 2 for an example on $q = 4$ nodes. The resulting DAG depicts a situation similar to that of a standard (Bayesian) probit regression model, wherein the covariates are not fixed but rather random and jointly independent with marginal normal distributions, $X_j \sim \mathcal{N}(0, \sigma_j^2)$, $j = 2, \dots, q$.

We then construct simulation scenarios as detailed in Section 6 of our paper. Results are summarized in the box-plots of Figure 3, where we report the distribution of the Mean Absolute Error (MAE, constructed across the 40 DAGs and nodes $s = 2, \dots, q$) under the two strategies as a function of n . As expected, our original method which fully accounts for the uncertainty on the DAG generating model, outperforms the alternative approach which is instead based on a fixed DAG not accounting for dependencies among variables. Indeed, it appears that the causal effect estimate significantly deviates from the true causal effect even for large sample sizes.

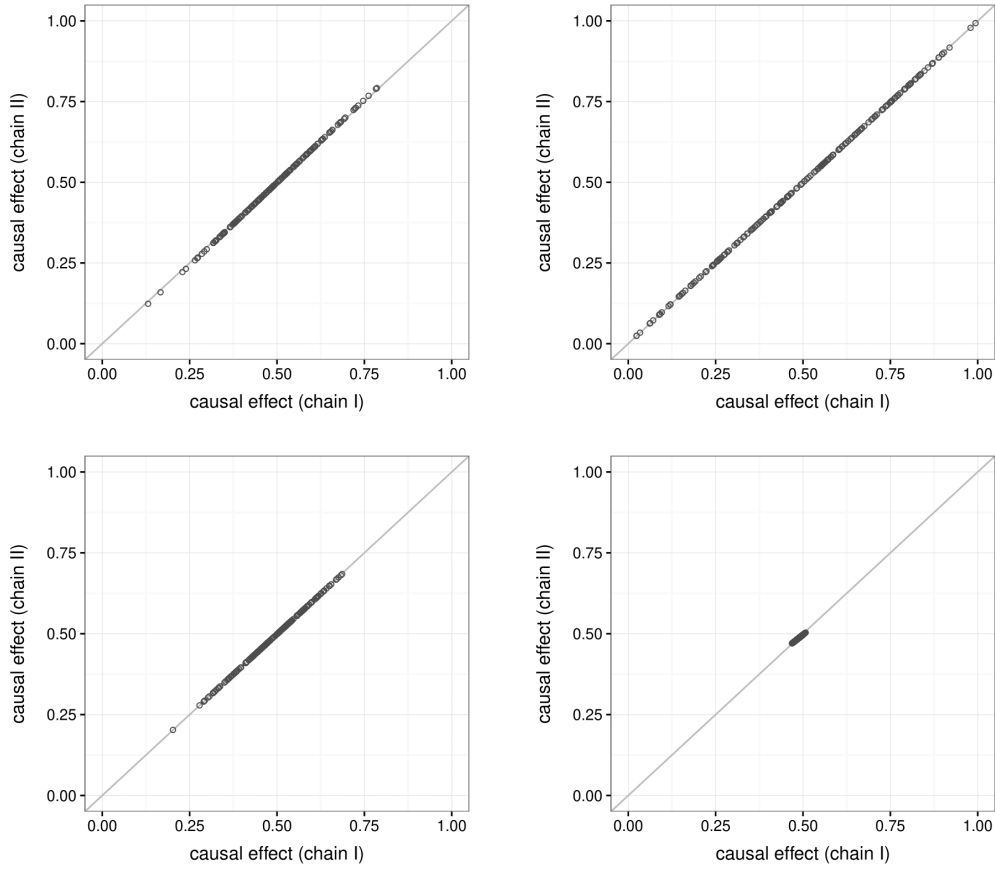


Figure 1: Scatter plots of the BMA estimates for four randomly chosen intervened nodes, obtained from two chains of length $T_1 = 25000$ and $T_2 = 50000$ (pilot simulation for the $q = 20$ setting).

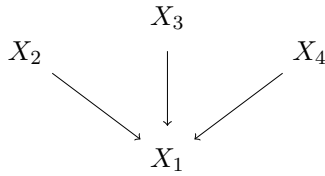


Figure 2: An instance of *naive* DAG with $q = 4$ nodes used in the alternative method under comparison.

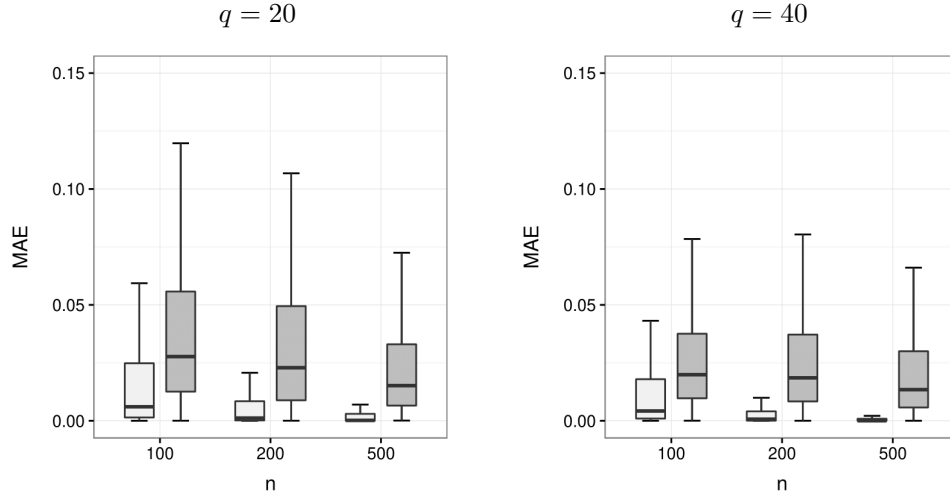


Figure 3: Distribution over 40 datasets and nodes $s \in \{2, \dots, q\}$ of the mean absolute error (MAE) of BMA estimates of true causal effects. Results are presented for two methods under comparison, our original DAG-probit method (light grey) and the *naïve* DAG-based approach (dark grey), for each combination of number of nodes $q \in \{20, 40\}$ and sample size $n \in \{100, 200, 500\}$.

6 Computational time

In this section we investigate the computational time of our method as a function of the number of variables q and sample size n . The following plots summarize the behavior of the running time (averaged over 40 replicates) *per* iteration, as a function of $q \in \{5, 10, 20, 50, 100\}$ for $n = 500$, and as a function of $n \in \{50, 100, 200, 500, 1000\}$ for $q = 50$. Results were obtained on a PC Intel(R) Core(TM) i7-8550U 1,80 GHz.

References

- GODSILL, S. J. (2012). On the relationship between markov chain monte carlo methods for model uncertainty. *Journal of Computational and Graphical Statistics* 10 230–248. URL <https://doi.org/10.1198/10618600152627924>. 3
- MELCHERS, R. E. & BECK, A. T. (2017). *Structural Reliability Analysis and Prediction*. John Wiley & Sons, Ltd. 8, 9
- WANG, H. & LI, S. Z. (2012). Efficient gaussian graphical model determination under g-wishart prior distributions. *Electronic Journal of Statistics* 6 168–198. URL <https://doi.org/10.1214/12-EJS669>. 3

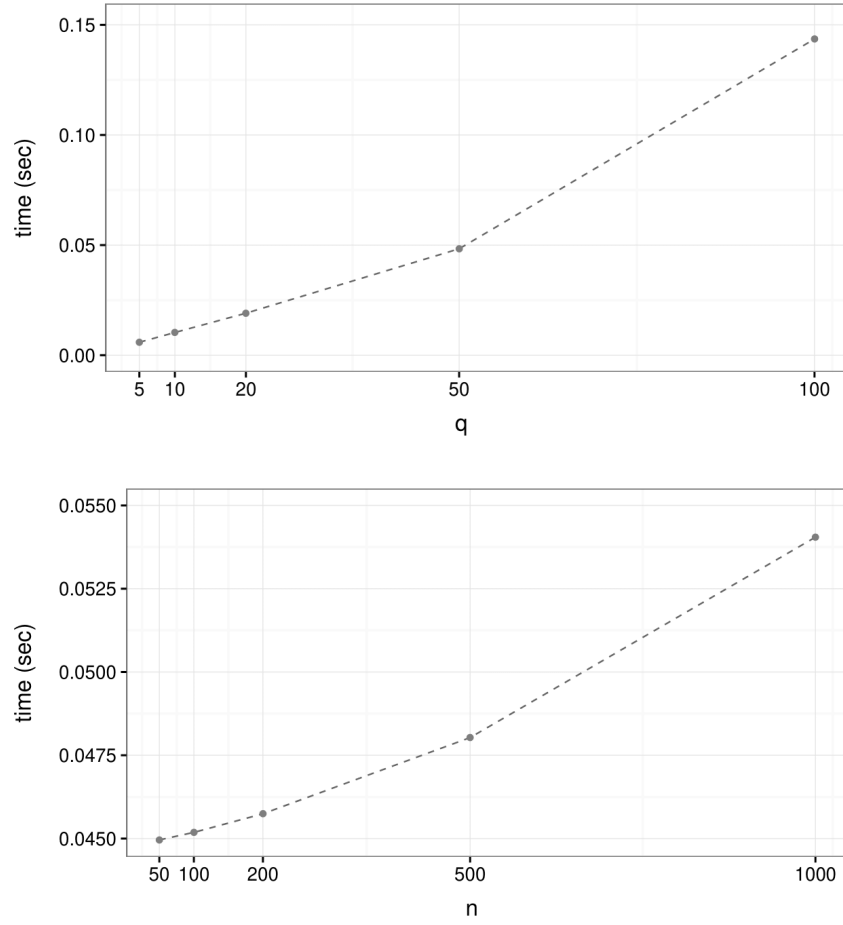


Figure 4: Computational time (in seconds) *per* iteration, as a function of the number of variables q for fixed $n = 500$ (upper plot) and as a function of the sample size n for fixed $q = 50$ (lower plot), averaged over 40 simulated datasets.